HEAT TRANSFER FROM THIN GOLD FILMS TO WATER IN SWIRLING FLOW

A THESIS

Presented to

the Faculty of the Graduate Division

by

Julian Denver Fleming, Jr.

In Partial Fulfillment

of the Requirements for the Degree

Doctor of Philosophy in the School

of Chemical Engineering

Georgia Institute of Technology

May 1959

"In presenting the dissertation as a partial fulfillment of the requirements for an advanced degree from the Georgia Institute of Technology, I agree that the Library of the Institution shall make it available for inspection and circulation in accordance with its regulations governing materials of this type. I agree that permission to copy from, or to publish from, this dissertation may be granted by the professor under whose direction it was written, or, in his absence, by the dean of the Graduate Division when such copying or publication is solely for scholarly purposes and does not involve potential financial gain. It is understood that any copying from, or publication of, this dissertation which involves potential financial gain will not be allowed without written permission.

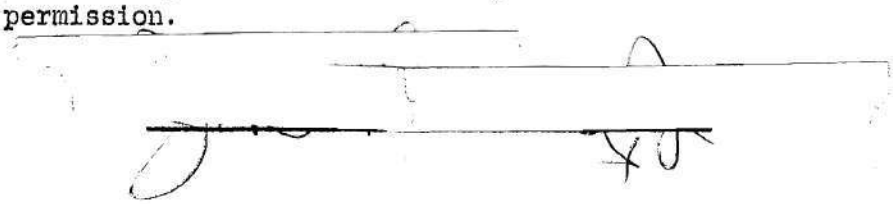

HEAT TRANSFER FROM THIN GOLD FILMS TO WATER IN SWIRLING FLOW

Approved:

Date Approved by Chairman: May 26, 1959

DEDICATION

This thesis is dedicated to the late Dr. J. M. DallaValle whose inspiration and friendship enriched everyone who knew him.

ACKNOWLEDGMENTS

The completion of this work is due to the combined efforts of many. The author is indebted to Dr. H. V. Grubb for his counsel, aid, and friendship; to Dr. W. B. Harrison who first aroused the author's interest in heat transfer; to Dr. H. C. Ward for his aid in completing the manuscript; to Mr. J. W. Johnson for his help with the thin films; and to Dr. Paul Weber for his continued guidance and counsel.

The gratitude of the author to his parents cannot be adequately expressed. Their active interest and participation through the years have been an inspiration without which this work would never have been done.

The author would also like to express appreciation to E. I. duPont de Nemours, Inc., for the Summer Research Grant which materially aided completion of this investigation.

TABLE OF CONTENTS

LIST OF TABLES

LIST OF FIGURES

SUMMARY

This study reports the development of high resistance gold film resistance heaters which can operate in high rate heat transfer processes with currents on the order of hundreds of amperes, rather than the thousands of amperes required for conventional systems. The suitability of the heating elements developed was tested in an exploratory study of heat transfer to water in swirling flow.

The advance of modern technology has resulted in the development of systems which are largely dependent, in size and performance, on the rate at which heat can be removed. Notable among these is the nuclear reactor whose size, for a given power output, is principally dependent not on nuclear considerations but on heat transfer capabilities. In a matter of only a few years, heat transfer engineers have jumped from heat exchangers operating by simple convection to equipment using liquid metals, boiling metals, molten salts, highly pressurized water, and fluidized beds, to mention only a few systems.

Since many of the new heat transfer processes involve extremely high heat fluxes and high temperatures, their laboratory investigation has become much more difficult. Conventional heating media such as steam and Dowtherm are

limited in the temperatures at which they can be used as well as the heat fluxes which they can furnish in simple use. As a means of avoiding these physical limitations, resistance heating with electricity has been extensively employed.

Although electrical power is theoretically unlimited in its ability to produce high heat flux and high temperature, its use introduces problems. Because of the low resistance of the metal tubes through which the coolants are circulated and with which the coolants are heated, the electrical sources are required to have low voltages and very large current capacities. The low voltages introduce errors from contact resistance unless metallurgical bonds are used throughout. The high currents require bulky and costly equipment and power lines.

This investigation records the development of a high resistance thin gold film heater with the ability to generate high heat flux and high temperature but with low current, high voltage electrical power. The test sections were Pyrex pipe spacers one inch inside diameter by two inches long. The spacers were coated on the inside with gold films, about 1200 Å thick, formed from Hanovia Liquid Bright Gold No. 5154. The coated spacers were soft-soldered to brass electrodes which were bolted to a water inlet and outlet supplying the spacers.

In order to investigate the suitability of the gold films as resistance test heaters in heat transfer studies, a brief investigation was made of heat transfer to water in swirling flow, a case which should severely test the corrosion and erosion resistance of the films. Square threaded, machined brass impellers with a range of blade angles were placed in the water inlet to the thin film test section to impart a tangential velocity component to the flow. The thin films were heated with 60 cycle AC power controlled by a saturable core reactor. The voltage drop and current flow were used to calculate the heat flux and the temperature of the films which were calibrated as resistance thermometers.

Heat flux curves were determined as a function of tangential velocity of the water up to burnout of the film. Water at $70^{\circ}F$ and, in most cases, not degassed, was used. The range of tangential velocities used was 20 to 80 fps. Axial velocities were 2 to 7.5 fps. Maximum currents and voltages were 225 amps and 80.4 volts. The film resistances at room temperature were of the order of 0.12 ohms. Burnout heat fluxes ranged from 1,420,000 to 3,600,000 Btu/hr ft^2.

Burnout did not follow the pattern noted with linear flow. Instead of reaching a critical burnout temperature difference at a low wall temperature, the films reached excessively high stable operating temperatures before burnout.

These temperatures were in the range of 1500°F. Burnout heat fluxes increased approximately with the square root of apparent tangential velocity.

The low slopes of the plots of heat flux as a function of wall-to-water temperature difference and the low burnout heat transfer coefficients were completely inconsistent with the mechanism of surface boiling. These observations were, at least qualitatively, consistent with forced convection. This would be the case if the water were moved radially away from the wall, under the high centrifugal acceleration arising from the tangential water flow, before being brought to the saturation temperature corresponding to the wall pressure.

The results of the study indicated that thin films can be used as resistance heaters in high level heat transfer studies. A need for further investigation was evident to concretely determine the conditions under which surface boiling can occur in high velocity swirling flow.

CHAPTER I

INTRODUCTION

With the introduction of high level power sources, such as nuclear reactors, the interest in more efficient heat transfer processes has steadily increased. The need for laboratory investigation of the high heat fluxes involved has severely taxed conventional experimental techniques.

This investigation records the development of a system utilizing thin gold films as resistance heaters and the application of the system to a brief study of heat transfer to water in swirling flow. The swirling flow case was chosen as placing the most stringent requirements on the gold films not only from the standpoint of heat transfer capabilities but also as to mechanical properties.

Historical Background

For many years, the heat transfer rates required for the successful design of engineering equipment were well within the limits afforded by low rate processes such as forced convection and simple boiling. Systems capable of transferring heat in excess of about 50,000 Btu/hr ft^2 were largely matters of academic interest only. Following

the Second World War, however, the development of high speed aircraft began to place demands on the heat removal capacity of existing systems. Government agencies began establishing programs, such as that summarized by Kays (1), with the objective of developing more efficient heat transfer systems.

The construction, in 1951, of the Experimental Breeder Reactor, the first nuclear reactor designed to generate power, opened a new era in the demand for heat removal systems of great capacity. The experience gained in the design and construction of this reactor firmly proved that, in a nuclear power reactor, "the power output is . . . determined essentially by the rate at which heat can be removed from the system." (2)

In investigating the new high level modes of heat transfer required for efficient operation of power reactors, the use of electrical systems to simulate actual operating conditions began to increase rapidly. The use of these systems, unlimited, in theory, in power generation capacity, temporarily satisfied the need for experimental systems. In order to obtain the desired levels of heat flux, however, extremely high amperage sources were required due to the low electrical resistance of the metal tubes used to contain and heat the coolants. Since both the equipment cost and technical difficulties increase with the required amperage, the need became obvious for experimental systems which would

have higher resistances and would thus be capable of developing large amounts of power at relatively low current.

Purpose of This Research

The need for a high power heat generation system, which would operate at low amperage, motivated this investigation. The electrical systems previously used placed rather strict limitations on the type of studies which could be made. In the resistance heating of fluid-carrying tubes, the low bulk resistivity of metals restricted the studies to small diameter, thin-walled tubes. In addition to this limitation, the contact resistance of the necessary connections was frequently of comparable magnitude with the resistance of the tube. As a result, complex joining techniques were required. The low voltages and high amperages involved were also difficult to measure accurately.

The only obvious way seen to alleviate some of these difficulties was the fabrication of resistance elements with much thinner walls, hence higher electrical resistance. Since the tubes utilized in studies by previous investigators were already thin enough to border on being mechanically unsound, a new approach was obviously required. This approach took the form of relying on a non-conducting material to furnish the necessary mechanical strength and forming a thin metal film, with a thickness of about 1200 Å, on the surface of the

non-conducting support to serve as the resistance element. By proper control of the thickness of the metal film, any desired resistance could be obtained.

Three main factors would control the range of application of such a system. First, in most flow systems a considerable amount of mechanical erosion would be expected at the wall of the tube; second, in such a thin film, corrosion by the coolant might be prohibitive; third, since the film would have limited mechanical strength, special methods would have to be developed for making electrical connections. The approach taken in the solution of the problem was initial development of the physical system, followed by testing the system in a swirling flow situation designed to emphasize the above factors.

Related Literature

Thin Films.--Thin metal films have been used for a wide variety of applications ranging from decoration of plastic parts to the formulation of reflecting surfaces for telescopes. These uses have been discussed in detail by Holland (3).

Thin films have recently been considered for use in resistance thermometry by Simpson (4), (5), and Winding (6). The negligible heat capacity associated with the films led the authors to suggest use of the films to accurately measure temperature transients. Chromium was found to form stable

films which were suitable for use over practical periods of time. The principal problem encountered by all of the above investigators was the change in resistance of the films during cyclic heating. This change in resistance has been noted in all films deposited by vacuum evaporation. This phenomenon was explained by Belser and Hicklin (7) as being due to annealing of the highly strained metal structure deposited by vacuum evaporation.

Swirling Fluid Flow.--Much work has been done on the swirling flow of compressible fluids (8), (9), (10). Even after many years of work by highly competent investigators, this system is only partially understood.

Not until recently was any significant study made of the swirling flow of imcompressible fluids. Talbot (11) studied the fluid motion resulting from a tangential swirl being superimposed on laminar flow in a round pipe. Binnie (12) made an experimental investigation of swirling flow of water in a nozzle. Again, these studies have failed to define completely the nature of the flow pattern.

Heat Transfer in Swirling Flow.--The idea of increasing the heat transfer coefficient in forced convection of im-compressible fluids was first proposed by Wollenberg (13) and Nagaoka and Watanabe (14). These authors considered the influence on heat transfer to water of swirl induced by twisted wires and strips. This study was revived and placed

on a more sound basis by Kreith (15), (16), who developed a theoretical relation for the effect of curvature on heat transfer and experimentally determined the influence of swirl on heat transfer to water. Kreith showed that the heat transfer rate was increased by the displacement of fluid from the heated wall toward the inside of the tube. The heat transfer was shown to be decreased for a swirling fluid flowing in an annulus and heated from the inside tube. This observation is of practical importance in that it shows that swirling flow is inapplicable in such situations as the cooling of rocket nozzle throats.

Gambill (17) reported an investigation similar in many respects to the present study. Gambill extended the study of swirling heat transfer to considerably higher tangential velocities than any of the preceding authors. This resulted in the increase of the heat transfer rate to the level of 55×10^6 Btu/hr ft^2. Gambill interpreted the results of his work in terms of the basic mechanism of boiling in swirling flow although, as was determined in this study, there is some reason to doubt the existence of boiling, prior to actual burnout, at the heat transfer surface in high-velocity swirling flow.

CHAPTER II

INSTRUMENTATION AND EQUIPMENT

In the design of the swirling flow system, the only problem of more than routine difficulty was the development of a suitable impeller to impart a tangential velocity component to the flowing fluid. Three criteria were established for the impeller section. The impeller should be capable of easy replacement to enable generation of flow patterns of varying tangential to axial velocity ratios. The velocity of the fluid in the impeller section should be kept as low as possible for a given mass flow rate so that the impeller pressure drop would be minimized. The flow pattern of the fluid leaving the impeller should be as well defined as possible.

The requirements of easy replacement and well-defined flow patterns effectively eliminated such impellers as spiral ramps and slotted injectors. A fluted, spiral impeller, fitted to the inside of a pipe, was chosen as the best means of meeting these criteria. In order to minimize pressure drop in the impeller, the spiral should have as few flow paths as would be consistent with structural and mechanical stability within the impeller.

First considerations indicated that the impeller which would give the lowest pressure drop would be one which gradually increased the tangential component of the fluid velocity. This would be accomplished by an impeller with blades which, if unrolled from the central cylinder, would describe a circular arc. Such a configuration cannot be produced by ordinary machining techniques. Milling asymmetrical shapes by chemical attack was investigated as a means of forming the desired impeller configuration.

Several aluminum alloys were investigated as base materials for the impeller. Various figures were cut into Scotch plastic tape No. 471 wrapped around cylinders of these alloys. These test specimens were immersed in solutions of hydrochloric acid in water, ranging in concentration from 5 to 30 per cent. The systems were allowed to react for periods of from 30 minutes to 14 hours while being continuously agitated at room temperature. The resulting etched shapes were examined for smoothness and uniform attack.

From the results of this preliminary study, 2-S aluminum was chosen as the most satisfactory for further investigation. A 15 weight per cent hydrochloric acid solution gave the best combination of uniformity of attack and speed. With this solution, a cut of 1/8-inch depth could be made in about 8 hours.

Impeller patterns were made by tracing overlapping circular arcs on strips of paper. These patterns were made 1/8-inch undersize on all sides to allow for undercutting during etching. These patterns were pasted onto 471 Scotch tape wrapped around 2-S aluminum cylinders which had been machined to 1-inch diameter. By cutting along the lines of the paper pattern, the tape was removed from the areas to be milled. The samples were threaded onto the shaft of a laboratory stirrer and immersed in the acid solution. The sample was turned by the stirrer at a slow speed, regulated by a Variac, and allowed to etch for 8 hours. The sample was then removed, the tape was stripped off, and the outlet end of the chemically milled impeller was turned down on a lathe to a point where the etched slots became most nearly tangent. The inlet side of the impeller was opened using a file.

An impeller was chemically milled using blade arcs with a radius of 5 inches. Three blades were used to provide sufficient holding points for this impeller when it was forced into a lucite pipe. Fewer than three blades allowed the impeller to work loose in the pipe as water was forced through it. The swirling flow pattern generated by this impeller in the lucite pipe was seen to oscillate in direction and to be generally unstable. This condition appeared to be due primarily to the inaccuracy involved in cutting the

pattern into the Scotch tape. Further attempts to eliminate this instability in the flow by using different methods of cutting the pattern, different numbers of blades, and different etching conditions met with little success.

In an attempt to generate a stable swirling flow pattern, a clean-up section was incorporated into the flow system. This clean-up section was made by turning a short section of a square-threaded screw on a lathe. The clean-up section was placed in the flow stream after the chemically milled impeller. The flow pattern leaving the clean-up section was stable and well defined.

Rough pressure drop measurements were made on the system using the chemically milled impeller together with the clean-up section and using the clean-up section alone. The pressure drop for the combination was slightly greater than for the clean-up section alone, indicating that the lower pressure drop resulting from the gradual change in the tangential velocity component was more than offset by the pressure drop caused by the friction in the chemically milled impeller.

Since the chemically milled impeller was difficult to produce and caused no improvement in the flow system, its use was discontinued and the impeller section was redesigned using only a machined, square-threaded impeller of constant pitch.

The square-threaded impeller, turned on the lathe, could be used with only one flow channel because of the small pitch. This served to decrease the velocity of the fluid in the impeller to a minimum for a given mass flow rate and thereby yield lower pressure drops. A section of about 1/2-inch length gave suitable support to be stable when shrink-fitted into a brass adapter. The lathe-turned impeller, however, was at a disadvantage in that the range of impeller blade angles was restricted to rather narrow limits.

In order to obtain a greater range of pitch angles, a standard vertical milling machine was modified to mill the impellers. A reduction gear-box was used with a small motor to drive a gear index head rather than having the gear index head turned by the mill bed gear system. This allowed the speed of rotation of the head and the impeller stock clamped in it to be altered at will for any bed speed. In turn, a wide range of impeller blade angles could be produced. Figure 1 shows an impeller being machined on the modified milling machine.

The impeller section was designed to allow the impeller itself to be changed readily. Impeller holders were machined, from brass stock, into which were shrink-fitted the milled, single-threaded impellers. The holder was machined to slip-fit into a brass pipe adapter. The impeller section is shown in Figures 2 and 3.

Four impeller assemblies were machined. These impellers are listed in Table 1. Each impeller was made as short as possible while still providing enough contact with the holding ring to be structurally stable.

The remainder of the flow system followed conventional practice and is diagrammed in Figure 4. Provision was made to take inlet water either from the water main or from a storage tank through a Viking rotary gear pump. The temperature of the water in the tank could be adjusted by circulating it through the auxiliary heater which was fitted for heating by steam or for cooling by water. After flow through the rotameters and downward through the vertical heating test section, the water was exhausted at atmospheric pressure to a catch tank from which it could either be discharged directly or returned to the storage tank for recirculation. Inlet and outlet water temperatures were measured with a Leeds and Northrup Model K precision potentiometer.

The associated electrical system is shown in Figure 5. The power source was a General Electric 125 kva saturable core reactor controlled by a rectifier regulated from the control panel. The voltages impressed across the test section were measured with a calibrated Heathkit precision vacuum tube voltmeter. The current flowing through the test section was read from three Triplett ammeters of different ranges. These ammeters were connected to current transformers in the

Table 1. Impeller Characteristics

Impeller	Slot Width (in.)	Depth (in.)	Average Blade Angle
B-18	1/8	1/8	$3^{\circ}30'$
B-14	1/4	1/8	$5^{\circ}50'$
B-38	3/8	1/8	$8^{\circ}35'$
B-12	1/2	1/8	$11^{\circ}10'$

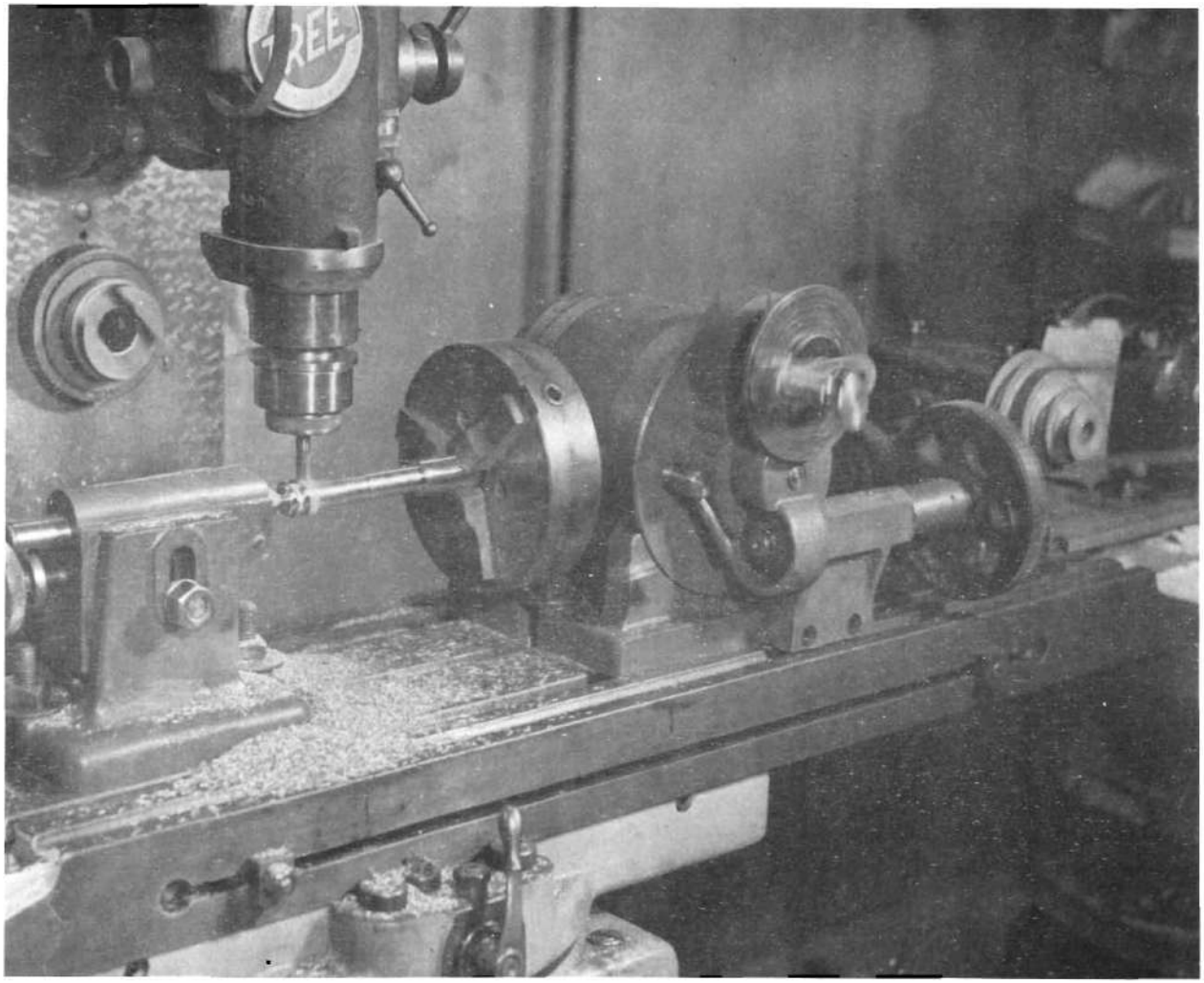

Figure 1. Impeller Being Machined.

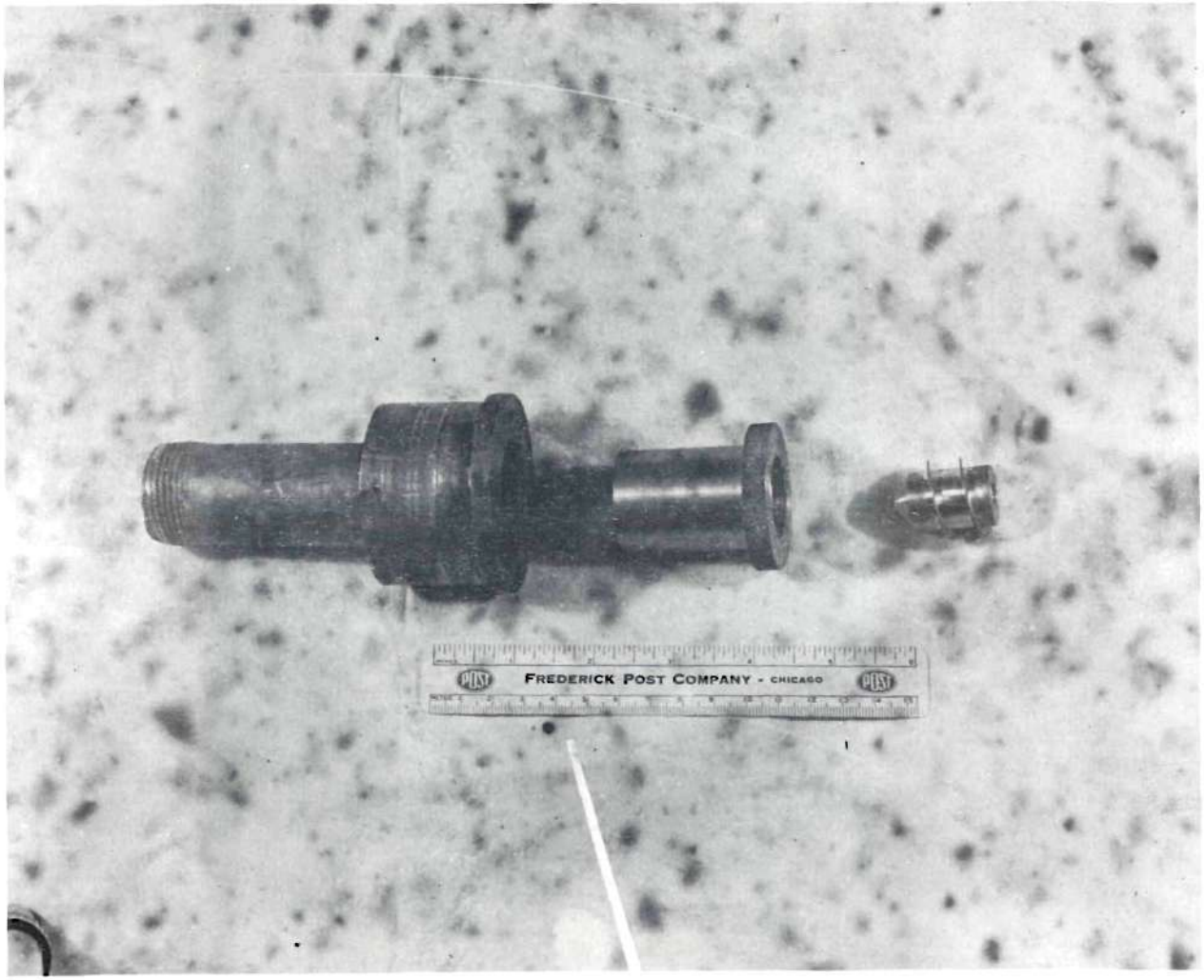

Figure 2. Impeller Section.

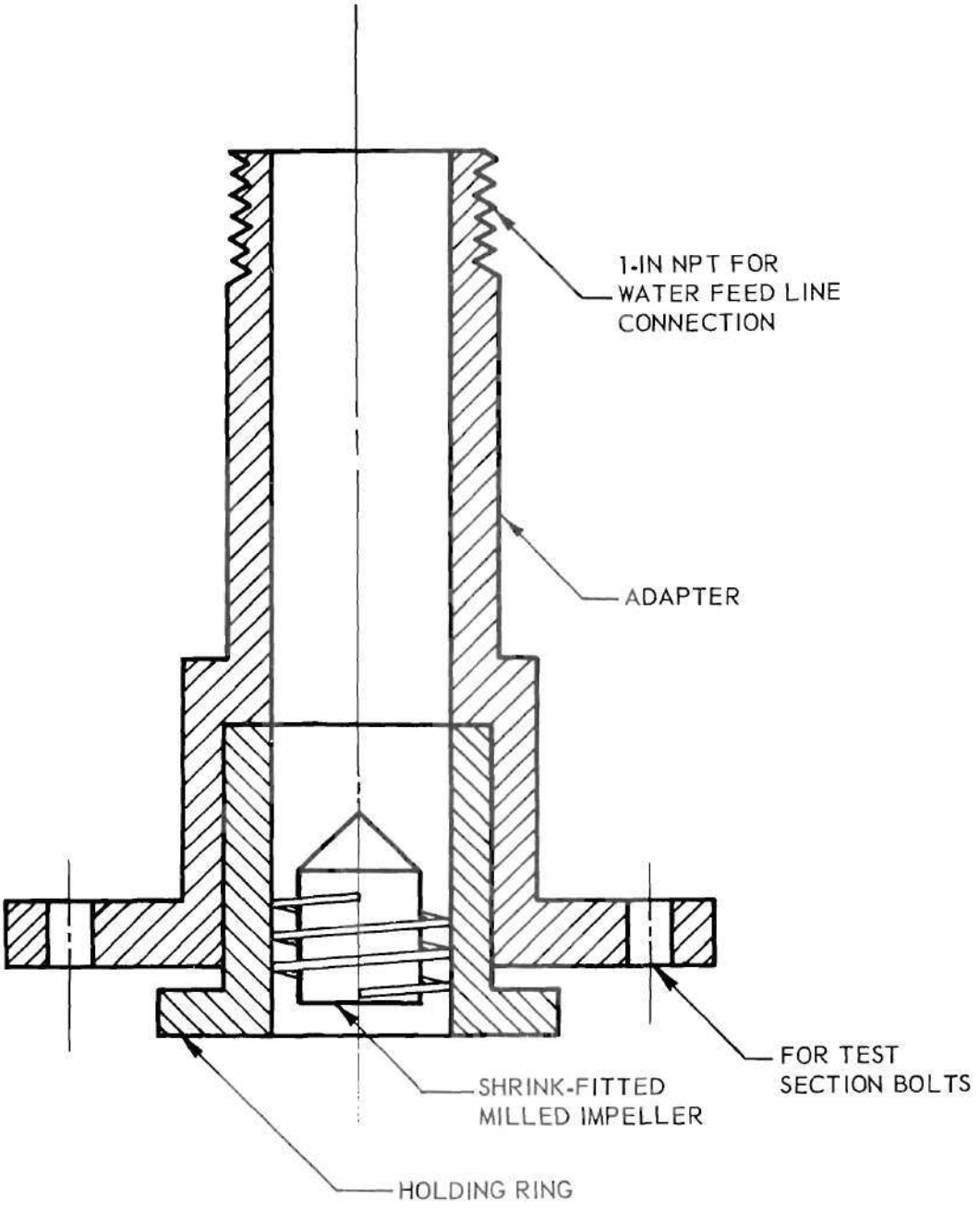

Figure 3. Assembled Impeller Section.

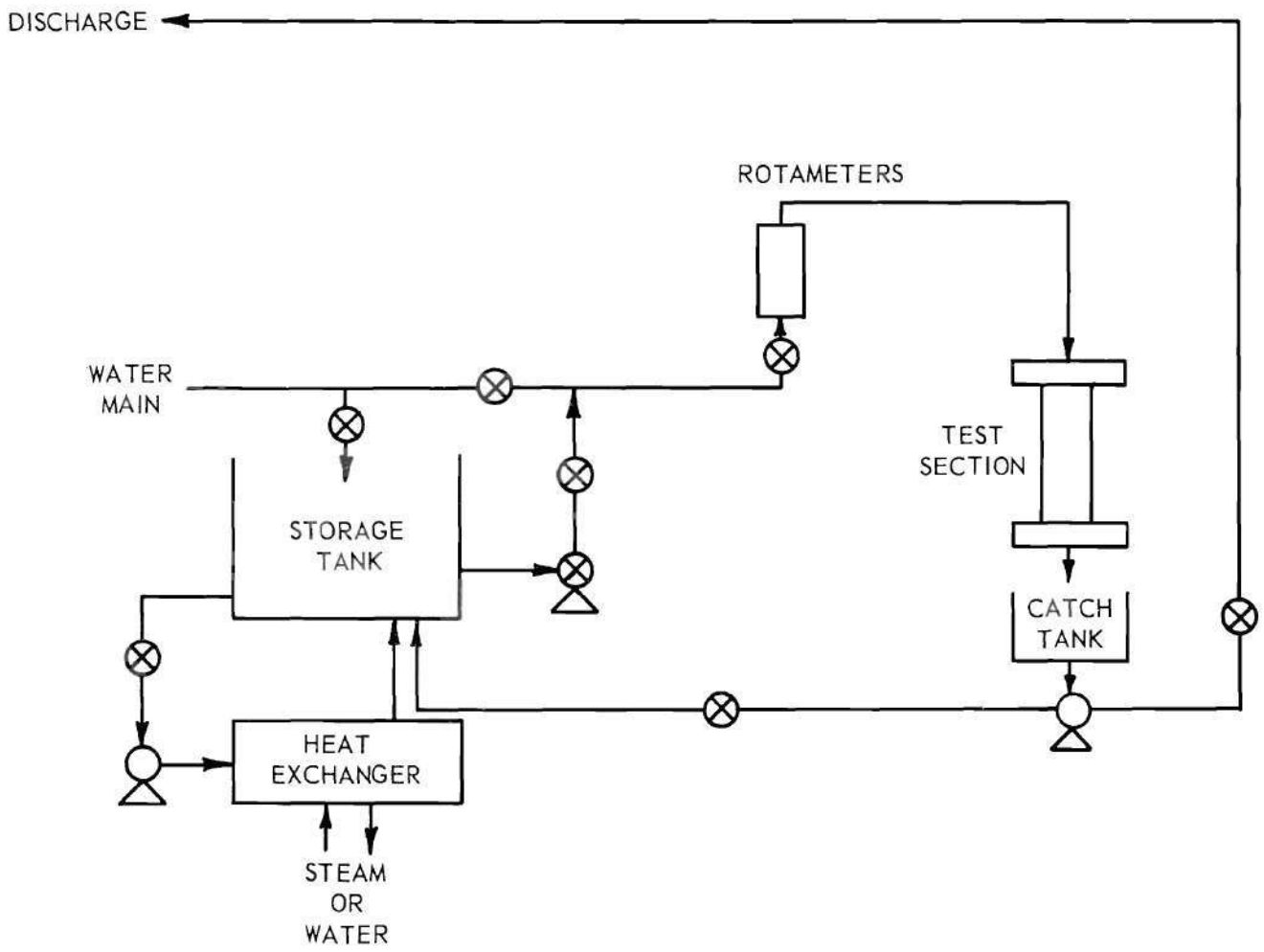

Figure 4. Schematic of Flow System.

power line. Either 600:5 General Electric or 200:5 Weston current transformers could be selected by changing electrical connections at the test section. A single 200:5 Weston current transformer was subsequently used in most of the tests since it was found possible to restrict the current flow to 200 amperes by proper control of the gold film thickness.

The saturable core reactor was shunted by a series inductor consisting of number 00 wire wrapped on a steel drum. The heating test section was connected in parallel with this inductor. The purpose of the inductor was to protect the heating test section from the initial current surge upon start-up of the reactor.

The heating elements were fabricated by soft soldering the coated 1-inch inside diameter by 2-inch long Pyrex spacers to ½-inch thick brass electrodes which could be bolted to the flow system. O-ring seals were used at the inlet and outlet joints of the test section. Solder joints could not be made directly with the gold films. To provide a basis for these connections, the ends of the gold-coated Pyrex spacers were painted with Flexible Silver, a highly conductive paste manufactured by the Hanovia Chemical Company. Following curing of these coatings, the silver was electroplated with copper. The electroplated copper layer could be soldered to the brass electrodes with ease. The resulting joints were capable of withstanding tensile loads

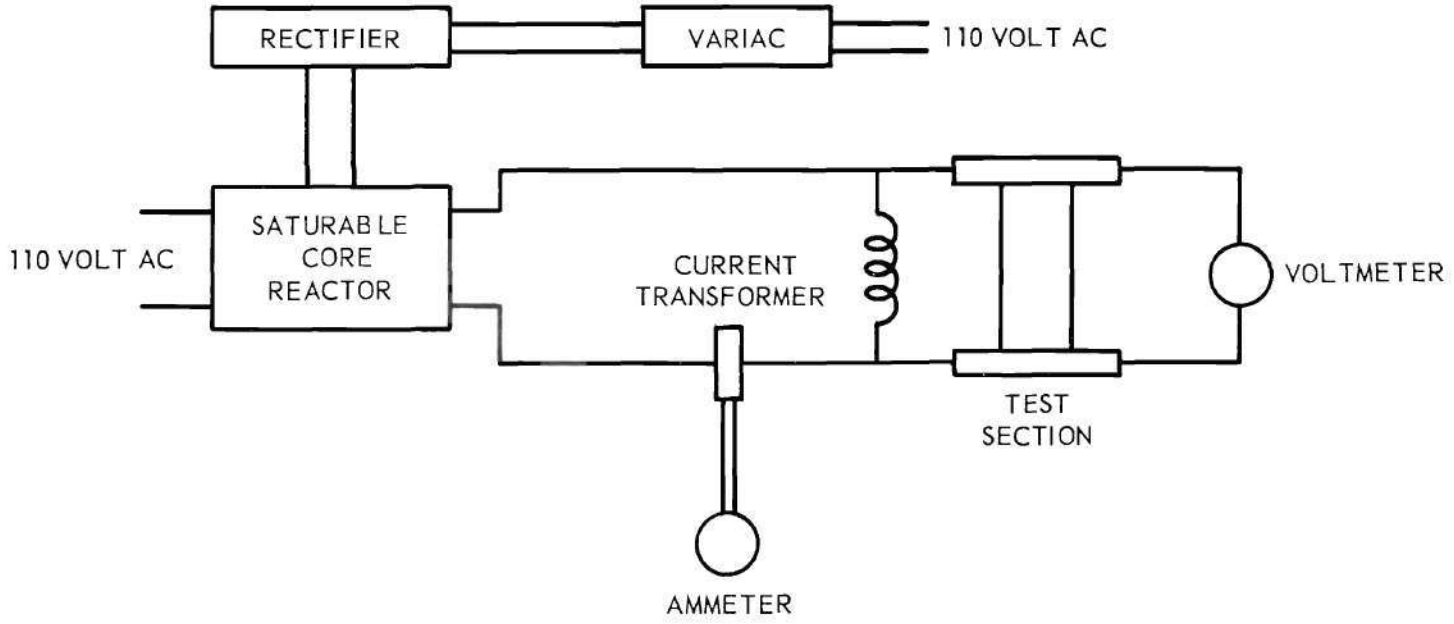

Figure 5. Schematic of Electrical System.

in excess of 50 pounds. The heating element and its relation to the flow system are shown in Figure 6.

The control panel is shown in Figure 7, and the overall test system is shown in Figure 8.

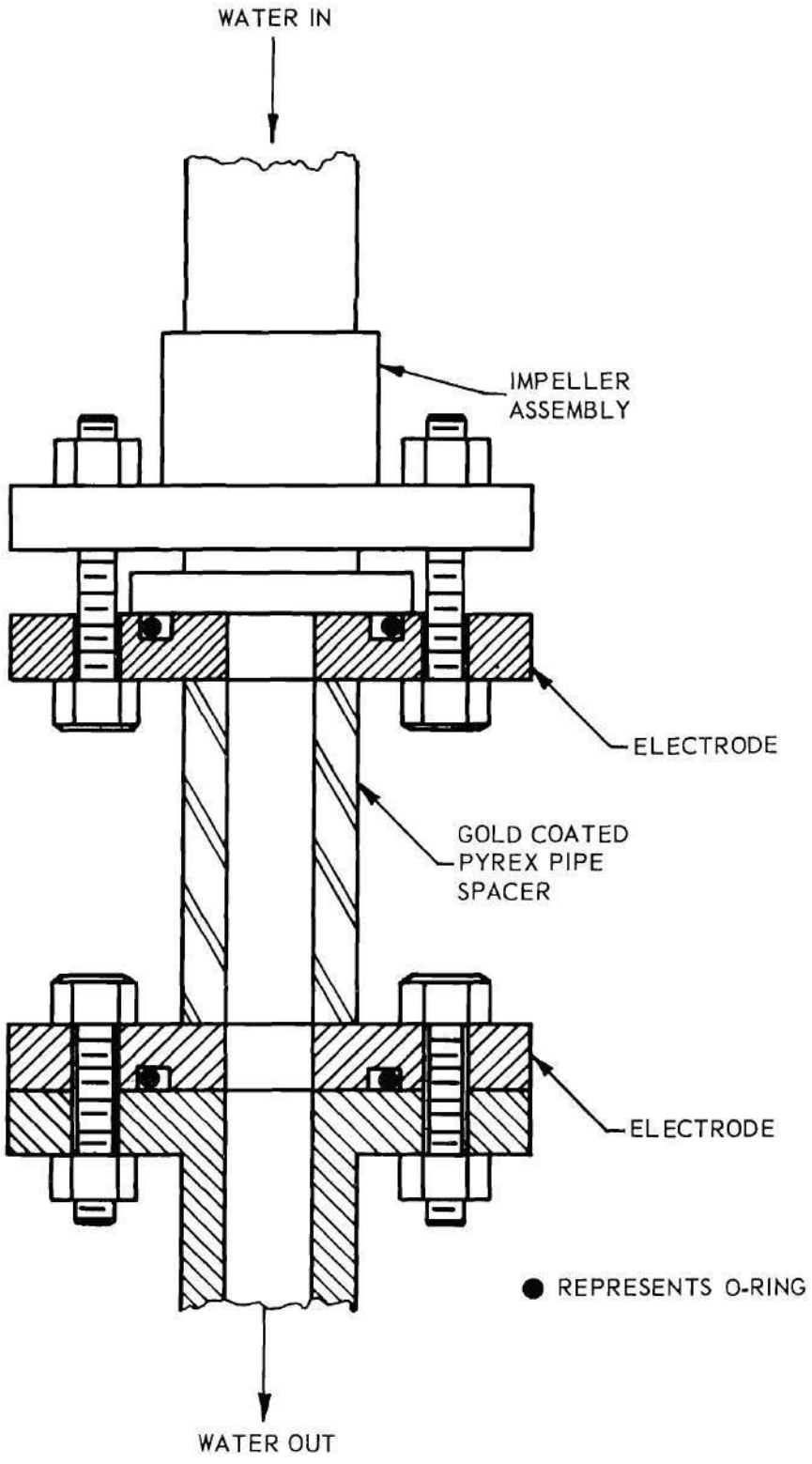

Figure 6. Test Section and Connections.

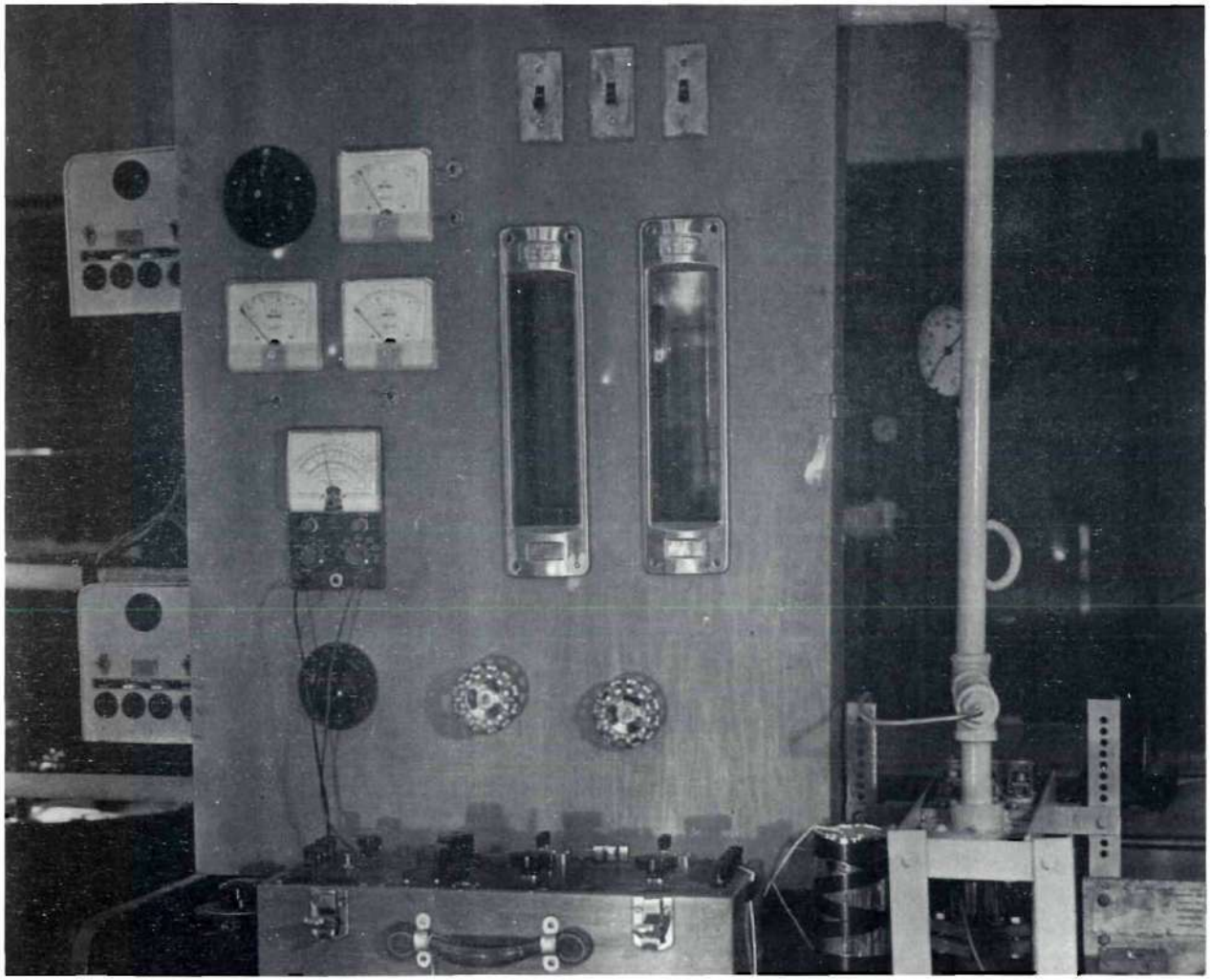

Figure 7. Control Panel.

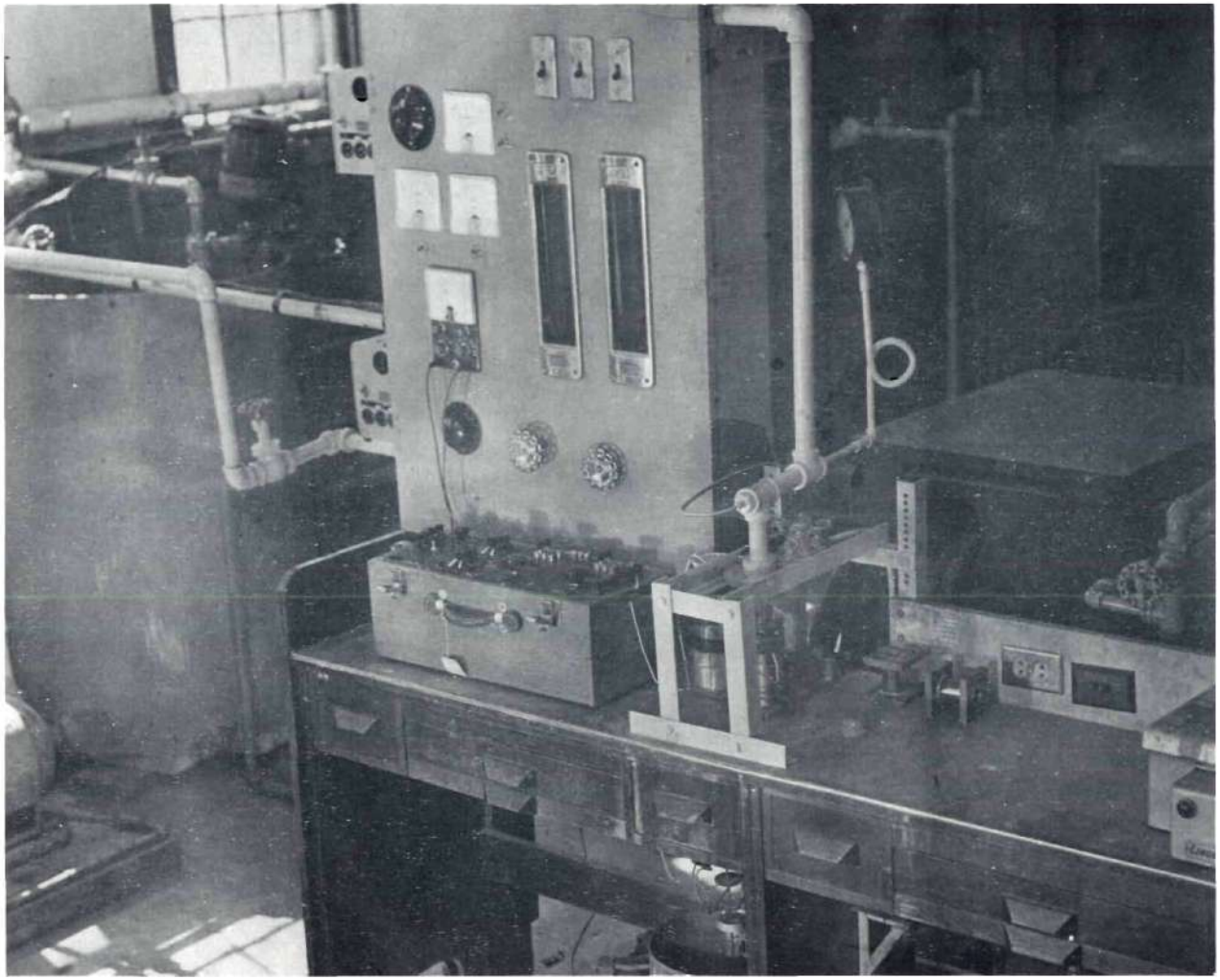

Figure 8. Test System.

CHAPTER III

PROCEDURE

Production of Heating Test Sections

The production of gold films by vacuum evaporation was first investigated. Utilizing standard techniques, thin films, 1200 Å or less in thickness, were deposited on the inside of 1-inch Pyrex pipe spacers by hot filament evaporation.

Prior to being coated, the spacers were scrupulously cleaned by the procedure of:

1. Flaming the surface
2. Scrubbing with Alconox detergent
3. Rinsing in distilled water
4. Immersing in aqua regia
5. Rinsing in distilled water
6. Scrubbing with Alconox
7. Rinsing in distilled water
8. Immersing in chromic acid cleaning solution
9. Rinsing in distilled water

Athough satisfactory coatings could sometimes be produced using a shorter sequence of cleaning steps, the lower percentage of rejects obtained from strict adherence to the above procedure made its use well worthwhile.

A clean tungsten filament was electroplated with gold, rinsed, dried, and placed in holding fixtures bolted to the electrodes of the evaporation system. The holding fixtures spring-loaded the filament to compensate for thermal expansion during the evaporation.

The system was pumped to a pressure of 10^{-4} mm. of mercury and the spacer was heated by the surrounding heater coil to drive off the adsorbed gases. This outgassing was found essential to the formation of adherent coatings. After the spacer was outgassed, AC power, controlled by a Variac, was fed to the tungsten filament until the gold was evaporated.

The gold films produced by the above procedure withstood the "Scotch tape test" in which Scotch cellophane tape is pressed onto the film and then pulled off. Failure of the Scotch tape to take the film off the substrate is a fair indication of good film adherence.

Since temperatures were to be measured by utilizing the films as resistance thermometers, a brief study was made of the effect of temperature cycling on the electrical resistance of the films. Evaporated films were found to undergo an irreversible change in room temperature resistance upon heating, probably due to a partial recrystallization of the highly strained crystal structure resulting from deposition by evaporation. The change in resistance destroyed

the usefulness of the films as resistance thermometers because of the concomitant change in the temperature calibration curve. This resistance change could be eliminated by heating the films to about 1100°F for two hours. This ageing process served to recrystallize the films. No difficulty was encountered in using the aged films as resistance thermometers.

Although the gold films could be successfully used as stable resistance thermometers, they were found to be incapable of resisting the erosion effects of the swirling flow. In a matter of only a few minutes, the films were stripped off the Pyrex spacer by the water flowing through the spacer.

The low adherence of evaporated gold films has been attributed to the presence of adsorbed gases on the surface of the substrate. The Hanovia Chemical Company produces a liquid gold resinate which can be coated on a substrate and then fired in air to produce an exceptionally adherent film. The firing process and combustion of the resinous components apparently are effective in purging the surface of adsorbed gases.

Trial samples were prepared from Hanovia Liquid Bright Gold No. 5154 and tested for erosion resistance in the flow system. These samples were found to show no evidence of mechanical erosion when subjected to swirling flow of the water for periods of several hours. In view of the

exceptional mechanical properties possessed by films produced in this manner, as well as the comparative simplicity of the necessary operations, all the films actually used as heat transfer elements were produced using the Hanovia compound.

The cleaning procedure which was used for preparing the spacers for coating by evaporation was also required in the sample preparation for fired gold coatings. One additional precaution was found necessary: the cleaned spacers had to be kept covered at all times to avoid having dust settle out on the surface of the spacers. The settling of any dust on the spacers, either before or after application of the Hanovia compound, invariably caused non-uniform and blotchy coatings to be formed on firing. The spacers were protected simply by being tightly wrapped in lint-free paper towels after they were cleaned.

After being cleaned, the spacers were held on a rubber stopper connected by glass and rubber tubing to a reservoir filled with the Hanovia Liquid Bright Gold. Compressed air was then admitted to the top of the reservoir, forcing the gold solution up into the Pyrex spacer. When the gold solution had completely filled the spacer, the air pressure was released from the reservoir and the gold solution was allowed to drain slowly back into the reservoir. A uniform, thin film of the gold solution was left behind on the surface of the spacer.

The coated spacers were dried for several days at room temperature. Any attempt to dry the samples faster through the use of higher temperatures frequently caused the film to become blotchy.

After the spacers had been thoroughly dried, they were packed into a tube furnace, through which air could be forced at a low rate. The spacers were then heated slowly and fired at 1200°F for 30 minutes. During the firing, the organic components of the gold solution were burned off, leaving behind a thin, continuous gold film. If the products of combustion were not removed rapidly by the flowing air, the coatings tended to blister during firing and be non-adherent.

With proper cleaning, exclusion of dust, and proper regulation of the air flow during the firing, satisfactory gold films could be conveniently formed as a routine operation by this method.

As a result of the high firing temperature used in producing the fired gold coatings, ageing of the films was found unnecessary. The resistance of the films was stable and did not change on heating.

Calibration of Heating Test Sections

Following production of the gold coated test sections but prior to their connection to the electrodes, the gold films were calibrated as resistance thermometers. The

resistance of the films was measured as a function of temperature using a Leeds and Northrup precision Wheatstone bridge. Temperatures up to about 212°F were obtained in a constant temperature water bath. Above this point, thermocouples were clipped to the elements and they were heated to just below the softening point of Pyrex (about 1250°F) in a laboratory furnace.

After being calibrated to 1200°F, the films were cooled to room temperature and the resistance was again measured. If any change was found in the room temperature resistance, the films were rejected.

Following the above calibration, the films were soldered to the brass electrodes. The assembled test sections were once more calibrated to 212°F in a water bath. The test sections were rejected if any deviation was noted from the preceding calibration.

The overall error arising in the temperature calibration of the films was $\pm 10^{\circ}$F.

In order to determine the effects of mechanical erosion on the temperature calibration, a heating test section was subjected to the highest flow rates available in the swirling flow system. During the test, the resistance of the film was continuously monitored. Over a period of three hours there was a resistance change amounting to an error in temperature measurement of $\pm 10^{\circ}$F. Since most of the heat

transfer tests were completed in less than half an hour of actual operating time, this error was deemed negligible.

A determination was made of the influence of chemical attack on the temperature calibration. A test section was boiled in water for four hours with continuous resistance monitoring. There was no detectable change in the resistance of the film during this test.

Heat Transfer Runs

In making a standard run, a heating test section was bolted to the flow system and the water flow rate was adjusted at the control panel. Following stabilization of the flow, the power switch to the reactor was closed, sending power through the shunting inductor. After the output of the reactor had reached a steady level, the hot electrode was attached to the test section. This procedure was followed to avoid premature burnout of the thin film due to current surges during the start-up of the reactor. In using metal tube test sections, this precaution is unnecessary because of the relatively high heat capacity of the tube. With thin films, having essentially no heat capacity, failure to observe this precaution almost invariably resulted in immediate burnout.

Following connection of the hot lead to the test section, readings were made of the voltage and current across the test section. The voltage was then gradually

increased with periodic readings being made up to the point of burnout of the test section. In some tests, only the burnout was to be determined so that no intervening readings were made.

As a result of the negligible response time of the thin film test elements, no difference was noted in burnout points whether the voltage was increased or, as is usually preferred, the water flow rate was decreased.

From the voltage and current readings, the heat flux, $\frac{q}{A}$, dissipated by the film could be determined from the relation

$$\frac{q}{A} = 3.41 \frac{EI}{A} \quad \frac{Btu}{hr ft^2}$$

where E represents the voltage, I represents the current, and A represents the surface area of the film (ft^2). The resistance, R, was calculated from

$$R = \frac{E}{I}$$

From the resistance values and the temperature calibration curves, the temperature of the film was obtained.

After familiarization runs were made and sources of difficulty were eliminated from the system, twelve runs were made in which sufficient information was obtained to make a plot of heat flux as a function of temperature difference

between the film and the water. Tap water at 70°F, which had not been degassed, was used in all these runs. Twelve runs were made with 70°F tap water, without degassing, in which only the burnout flux was determined. Two runs were made with 70°F water which had been degassed by boiling in order to investigate the effect of dissolved air on the burnout flux.

CHAPTER IV

RESULTS AND DISCUSSION

Production of Film Heating Elements

Once the technique of gold film deposition was developed, production of satisfactory heating test sections proceeded routinely without further difficulty. The primary problem associated with this aspect of the study was simply the gaining of enough experience to handle the coating method with some degree of facility. The techniques developed may be quantitatively described as in the preceding chapter, but the uninitiated investigator should not expect to be able to produce a satisfactory film the first few times, even by rigidly adhering to the procedure given. Anyone wishing to carry out work using test sections similar to those developed in this investigation should expect to spend a minimum of several weeks merely acquiring the talent for forming suitable films.

In order to form films with room temperature resistance values in the range of 0.1 to 0.3 ohms, from three to five cycles of coating and firing were required. The attempt to form thick films in a single dipping invariably led to blistering and peeling of the coating. The necessity for

repeated coatings resulted in about two weeks of elapsed time being required for the fabrication of a test section. As a result, an inventory of Pyrex spacers was necessary. The expense associated with this inventory was decreased by the fact that the spacers could be repeatedly re-used after the gold films and end coatings were stripped off with nitric acid and aqua regia solutions.

The films finally produced in this study proved quite stable with respect to resistance changes during temperature cycling. During the entire test run program, only two films were rejected because of resistance changes during calibration.

Mention should be made of the fact that the films produced just bordered on opacity. Had the voltages used been allowed to approach 110 volts, the limit of the saturable core reactor, sufficiently thin films could have been used to allow observation of the wall phenomena occurring in the test section. This technique was considered for use but was discarded because the high turbulence at the free liquid interface, resulting from the swirling flow, obscured visual observation. In more conventional systems, such as boiling in linear flow, the technique of visual observation of wall phenomena might prove highly useful. Even in swirling flow, techniques might be developed to minimize the optical effects of the free liquid interface. Such a development would be of great interest for reasons to be stated later.

The gold films used as resistance heaters had a mass of only about 10^{-5} pounds. This low mass, and consequent negligible heat capacity, resulted in the response time of the resistance heater being differentially small. This fact was of over-riding importance in the manipulation of the test equipment and the subsequent interpretation of the results.

The first effect of this negligible response time was the production of immediate burnout if the reactor was activated with the test section connected. This problem was successfully solved by the use of the shunting inductor previously mentioned. A far more serious aspect of the same problem was the inadequacy of the conventional instrumentation used. Small fluctuations in the flow pattern of the water resulted in the immediate heating or cooling of the gold film with concomitant resistance changes. These resistance changes caused an essentially continuous fluctuation in the electrical meter readings. These fluctuations introduced an inaccuracy of roughly five per cent in the meter readings. The influence of this inaccuracy may readily be evaluated from considering that a five per cent error in the resistance of the film represents an error of better than $100^{\circ}F$ in the temperature determinations. This error must be kept in mind in viewing the quantitative accuracy of the results obtained. Since the film responds so rapidly, the only way to eliminate the error in temperature determination would be through the use

of high speed oscillographs. This type of instrumentation would also be valuable in concretely evaluating some of the factors to be stated later.

Heat Transfer Experiments

The values of heat flux, calculated from the electrical measurements, were found to follow approximately a straight line relationship with the temperature difference between the film and the water when plotted on logarithmic grid paper. The experimental and calculated data from the experiments are given in Appendix A. The curves of heat flux as a function of temperature difference are given in Appendix B.

The slope of the heat flux curves was noticed to increase slightly with water velocity. The runs were made in such a way that information could be obtained on the influence of increasing tangential velocity at closely constant axial velocities. This was accomplished through the use of the impellers with different blade angles listed in Table 1. The runs fell into four groups of approximately constant axial velocity as shown in Table 2.

The velocities shown in Table 2 and the velocities mentioned elsewhere in this report are apparent velocities only. These values were calculated from the mass flow rate, the known area of the impeller slot, and the angle of the impeller blade. The velocities calculated in this manner thus represent the velocities possessed by the fluid stream

Table 2. Tabulation of Water Velocities Used

Run	Impeller	Axial Velocity	Tangential Velocity
		(ft/sec)	(ft/sec)
21	B-18	2.0	32.0
9	B-14	2.0	19.5
18	B-18	3.2	49.0
4	B-14	3.2	32.8
13	B-38	3.1	20.5
19	B-18	4.9	80.0
15	B-14	5.0	48.9
7	B-38	5.1	34.0
22	B-12	4.9	25.2
10	B-14	6.7	66.0
2	B-38	6.7	44.6
14	B-12	7.3	37.5

if it underwent no change in direction or size in leaving the impeller and are, therefore, only rough approximations.

No well defined influence of axial velocity on the slope of the heat flux curves could be discerned. The slopes of the curves obtained from the runs of Table 2 are shown as a function of tangential velocity in Figure 9. The straight line drawn in the figure was fitted by the method of least squares and correlates the data with average and maximum deviations of 1.8 and 5.4 per cent respectively.

Although Figure 9 does show a qualitative trend, no quantitative significance can be attached to it. This is well demonstrated in that the points plotted therein differ from their common average by an average and maximum of only 3.4 and 9.3 per cent respectively. In addition, the temperature differences used in the curves from which the slopes were obtained have been shown to be reliable within no more than $100^{\circ}F$. Coupled with the fact that reading slopes from graphs having the scatter noted is of only limited precision, the above facts show the degree of correlation to be entirely fortuitous. No equation was determined for this line in order to at least inhibit the casual reader from extrapolating the trend, expecting to obtain quantitative results, to a region where it almost certainly is inapplicable.

The burnout fluxes for the experimental runs were calculated by doubling the flux calculated from the

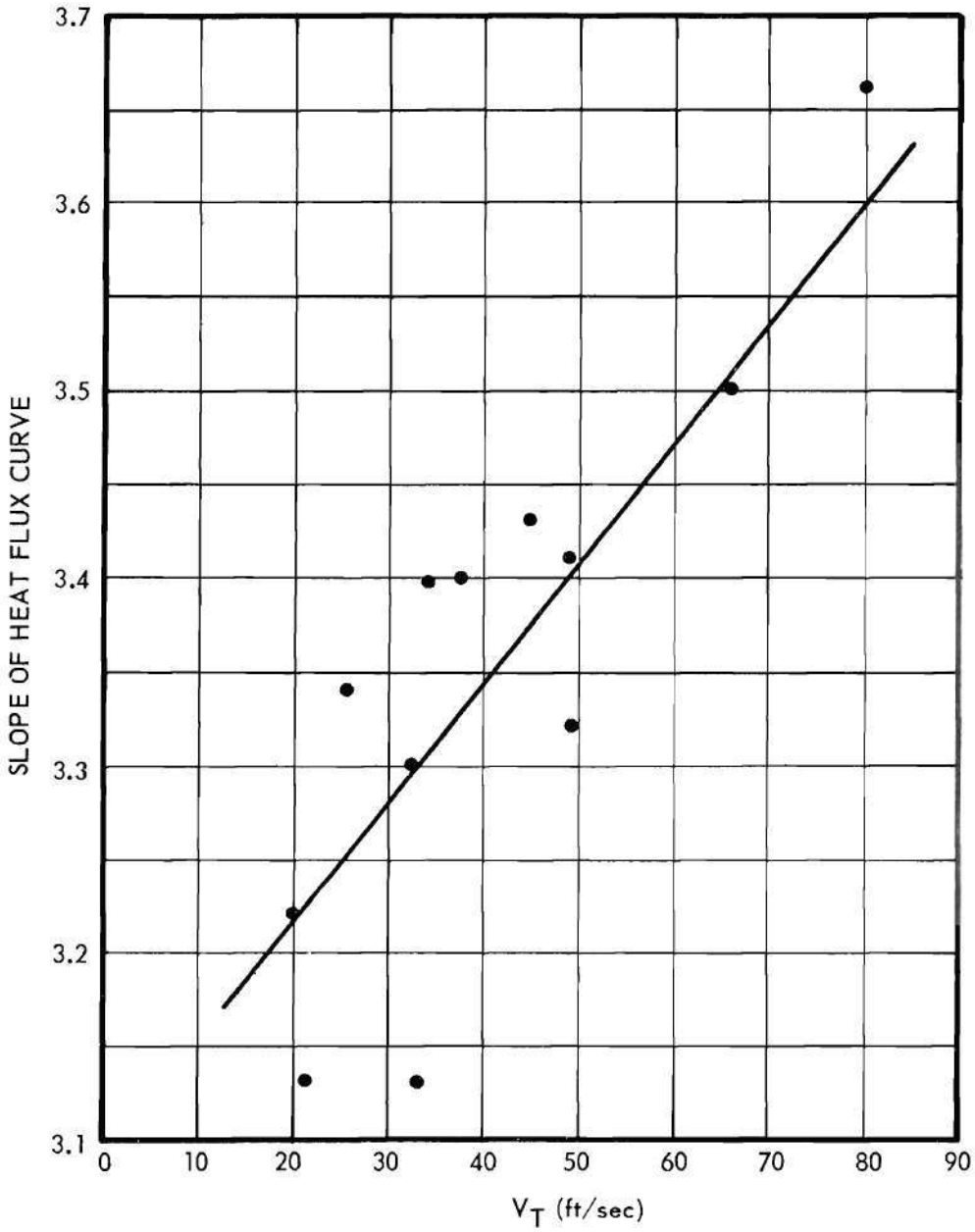

Figure 9. Slope of Heat Flux Curve as a Function of Apparent Tangential Velocity.

electrical meter readings at the time of burnout. The reasons for this apparently arbitrary procedure will be discussed in the mathematical procedure to follow. Again no correlation with axial velocity was apparent. The results of all the runs made have, therefore, been plotted in Figure 10 as a function of tangential velocity. The straight line drawn in Figure 10 was fitted by the method of averages and has the form

$$\left(\frac{q}{A}\right)_b = 2.93 \times 10^5 \, V_T^{0.558} \qquad (1)$$

where $\left(\frac{q}{A}\right)_b$ is the burnout heat flux $\left(\frac{Btu}{hr\,ft^2}\right)$ and V_T is the apparent water tangential velocity (ft/sec). Equation 1 fits the burnout data with average and maximum deviations of 6.3 and 12.5 per cent respectively.

Because of the errors associated with the temperature measurements, the heat flux curves were somewhat scattered on the temperature axis. In view of these uncertainties, no general equations were developed to try to correlate all the data.

The burnout temperatures were determined by extrapolating the heat flux curves to the calculated heat flux at burnout and reading the corresponding temperature. This technique was employed as a consequence of the mathematical treatment to follow. No correlation or trend was evident in

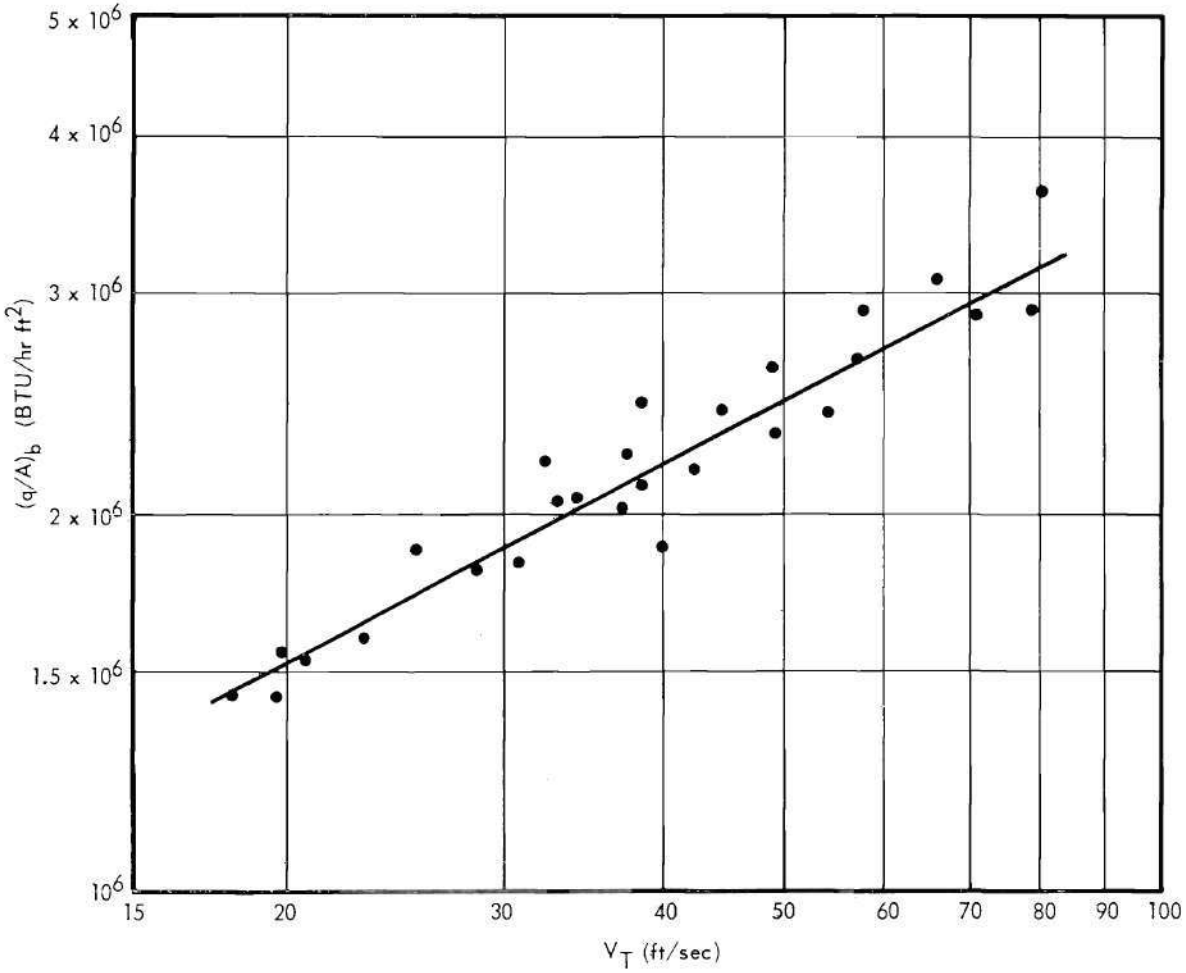

Figure 10. Burnout Heat Flux as a Function of Apparent Tangential Velocity.

the burnout temperatures. The values ranged indiscriminately from 1320°F to 1930°F with an average of 1650°F.

Calculations were made at intervals of the heat flux from the measured water inlet and outlet temperatures and the water flow rate. These values usually checked those from the electrical readings within five per cent.

The dissolved air had no profound influence on the burnout flux in the runs made. Runs number 3 and 5 were made with water which was degassed by boiling and cooled to 70°F. These runs were made at essentially the same flow conditions and gave an average burnout flux of 2,230,000 Btu/hr ft^2. Runs 6 and 14 were made at almost the same conditions with water which was not degassed. These runs gave an average burnout flux of 2,170,000 Btu/hr ft^2. This result is consistent with the mechanism of swirling flow in that the centrifugal acceleration imparted by the tangential velocity component would force any air bubbles away from the wall. In the absence of blanketing of the heat transfer surface by free air, the burnout flux should be unaffected.

Discussion of Results

The heat transfer runs were organized and carried out with the full expectation of the basic heat transfer mechanism being boiling. In fact, the idea of heat being transferred to water, in contact with metals at temperatures well in excess of 500°F, by any mechanism other than boiling seemed

faintly ridiculous. Initial compilation of the data during the runs failed to indicate anything erroneous in this thinking since the burnout heat fluxes were of the same order of magnitude as those for surface boiling burnout commonly reported in the literature. Not until the final results were compiled did any doubt arise concerning the wall phenomena in the system.

The first clue noted was that the slopes of the heat flux curves were only about half the value to be expected from surface boiling of subcooled water. A second indication was that an examination of the heat transfer coefficients at burnout showed them to be on the order of 1000, a full order of magnitude lower than those usually associated with surface boiling. Still a third, somewhat less conclusive indication was the complete absence of any singing or popping noises at any point in the runs. These noises are quite common in surface boiling and usually begin at heat fluxes from half to three quarters of the burnout flux, presumably occurring during the growth and collapse of bubbles at the heat transfer surface. Gambill (17) noticed the same absence of noise in his experiments and attributed it to the presence of the free liquid surface in the center of the swirling fluid. This explanation is very unlikely since the same noises occur in surface boiling of subcooled water in shallow pools with great free surface areas. Gambill determined that boiling occurred in his experiments only through determination

of the point at which the tube wall temperature reached the saturation temperature of the water at the measured wall pressure of the tube. This criterion is not adequate for asserting that boiling occurred for reasons to be developed below. Gambill stated that Oppenheimer (Nuclear Development Corporation of America) and Bonilla (Columbia University) have also carried out unpublished investigations of boiling in swirling flow. No statements were made as to how these investigators established the existence of boiling in their experiments.

Once these observations were grouped together, the occurrence of boiling at the surface of the heating element became open to serious doubt. A few rough calculations increased the doubt that boiling occurred. The tangential velocities used in this investigation resulted in calculated centrifugal accelerations in the fluid stream between about 8,000 and 100,000 ft/sec^2 or from about 300 to 4,000 times the normal acceleration of gravity. As a result, the Grashof numbers, characteristic of the buoyant forces acting on fluids, became about 10^{15} whereas Grashof numbers of about 10^9 are sufficient to cause turbulence in natural convection. A more striking example is shown by the calculation of the buoyant forces acting on a particle of heated water at the tube wall under the centifugal acceleration encountered in the mildest flow conditions used in this investigation.

Taking a tangential velocity of 20 ft/sec, the centrifugal acceleration becomes, roughly,

$$a = \frac{V_T^2}{R} \doteq \frac{(20)^2}{(\frac{0.5}{12})} \doteq 9600 \frac{ft}{sec^2}$$

If the water at the wall is assumed to be at 150°F and the bulk water temperature is assumed to be 70°F, the buoyant force on the water becomes

$$f = m\frac{a}{g_c} = \frac{a}{g_c} (\rho_{70} - \rho_{150})$$

$$\doteq \frac{9600}{32.2} (62.3 - 61.2)$$

$$\doteq 329 \quad \#f/ft^3$$

The full impact of this result will be realized by comparing it with the buoyant force on a steam bubble liberated in ordinary boiling at 212°F.

$$f \doteq \frac{32.2}{32.2} (60)$$

$$\doteq 60 \quad \#f/ft^3$$

The buoyant forces acting to displace the heated water from the tube wall are thus seen to be <u>better than five times</u> those displacing steam bubbles in ordinary boiling. Under these

circumstances, there is a very good possibility that the water could be removed from the wall before it reached the saturation temperature.

While the above facts certainly do not conclusively prove that boiling does not occur at the wall in swirling flow, they do make the statement more reasonable. The compilation of these facts, in the absence of any direct visual observation of boiling, forces the conclusion that the heating occurred by convection with strong radial fluid transport resulting from the centrifugal forces imposed by the swirling flow.

A conjecture may be made on the basis of this conclusion as to the behavior of the water in the swirling flow system. As the cold swirling water comes into contact with the hot wall, it is heated and displaced by the buoyant forces arising from the high centrifugal acceleration imparted by the swirling flow. The displaced hot water is immediately replaced by colder water from the bulk fluid stream and the cycle is repeated. If the heated water does not mix rapidly enough with the bulk cold water and if its temperature is high enough, it may flash into steam at some critical position where the radial pressure gradient in the stream has caused the fluid pressure to drop to the saturation point for the heated water. If this critical point is far from the heating surface or if the quantity of water flashing is small, the

vapor will probably recondense in the bulk stream with no serious effects. As the velocity is decreased, or the wall temperature is increased, this critical pressure point will move closer to the wall because of either decreased pressure gradient or increased water temperature. At some time, the quantity of water flashing to vapor will be large enough and the flashing point will be close enough to the wall to choke the flow of cold water to the wall. The water at the wall will then be explosively vaporized, steam blanketing of the heating surface will occur, and burnout will follow.

If the picture drawn by the foregoing statements is correct, surface boiling prior to burnout would be even less likely to occur with higher tangential velocities. If this is true, heaters should be capable of operating near the melting point of the heater metal with radically increased heat fluxes resulting. In this investigation, since the film temperatures were, within experimental accuracy, close to the melting point of the gold, no statement can be made as to whether the burnout occurred by vapor blanketing of the heating surface or merely because the operating temperature reached the melting point of gold. It is conceivable that the limiting heat flux, without vapor binding, was not actually reached in this experiment. The use of a higher melting metal film should then permit greater heat fluxes to be attained in the same system.

While the preceding discussion is rather coarse, no more sophisticated approach may be intelligently taken with the limited data on hand. Too much emphasis cannot be placed on the fact that conventional theories and pictures of fluid flow simply do not apply to the case of swirling flow. With wall heating, and consequent radial fluid transport, the swirling flow is thrown into the category of three dimensional fluid flow. Tangential, axial, and radial flow components must be expected. Under these circumstances, no logical basis can be selected for comparison of swirling flow with ordinary linear flow. Without more information on the mechanisms of swirling flow and heat transfer, no calculation can be made of a quantity, such as a hydraulic diameter or Reynolds number, which would have any real significance.

Mathematical Treatment

Since AC power was used in conjunction with thin films having essentially zero response time, some interesting phenomena could be expected to occur in the heat transfer systems. Two occurrences of great significance were predicted from elementary mathematical treatment. Since the results of this treatment were used in interpreting the results of the heat transfer runs, a consideration of the mathematical development is in order here.

Influence of AC Heating

In a metal cylinder being heated with AC power, temperature fluctuations would be expected in the metal because of the cyclic variations in heat generation rate. Some conclusions may be drawn concerning the magnitude of the temperature fluctuation based on the following assumptions:

(a) Negligible radial and axial temperature gradients in the cylinder.

(b) Power generation dependent only on time, not on position.

(c) Electrical and thermal properties independent of temperature.

(d) Constant heat transfer coefficient from the interior surface.

(e) Perfectly insulated on the exterior surface.

(f) Constant environment temperature.

Based on these simplifying assumptions, q_t, the rate of heat transfer from the interior surface of the cylinder at any time, θ, is given by

$$q_t = hA(t_s - t_e) \qquad (1)$$

in which h is the heat transfer coefficient, A is the interior surface area of the cylinder, t_s is the surface temperature, and t_e is the environment temperature. If the temperature difference between the surface and the environment,

$$T = t_s - t_e, \tag{2}$$

is substituted, Equation 1 becomes

$$q_t = hAT \tag{3}$$

dQ_t, the amount of heat transferred in the time interval $d\theta$ is given by

$$dQ_t = hATd\theta \tag{4}$$

The heat stored in the cylinder during the time $d\theta$ because of the accompanying temperature increase is

$$dQ_s = mCdt_s \tag{5}$$

where m is the mass of the cylinder and C is its specific heat capacity. Since

$$T = t_s - t_e$$

from Equation 2,

$$dT = dt_s \tag{6}$$

and

$$dQ_s = mCdT \tag{7}$$

Since the voltage impressed on the cylinder is a sinusoidal function of time and since the resistance of the cylinder

has been assumed constant, the power generated in the cylinder will be a sinusoidal function of time. Because the instantaneous power, p, is given by

$$p = \frac{E^2}{R}$$

where E is the instantaneous voltage and R is the cylinder resistance, the frequency of the power fluctuation will be twice that of the voltage fluctuation. In the case of a 60 cycle voltage, the power follows a 120 cycle sine wave. Since the power generation is related to the heat generation by a numerical constant, the heat generation will also follow a 120 cycle sine wave. If this sinusoidal function is stated so that the instantaneous heat generation rate, q_i, is equal to the average heat generation rate, q, at a time, θ, equal to zero, then

$$q_i = q(1 + \sin 2\pi f\theta) \qquad (8)$$

where f is the frequency of the sinusoidal heat generation rate. Attention should be paid to the fact that the units of frequency and time must match in this relation. If θ is stated in hours, then f must be stated in cycles per hour. If

$$w = 2\pi f \qquad (9)$$

Equation 8 becomes

$$q_i = q(1 + \sin w\theta)$$

and the heat, dQ_g, generated in the time interval $d\theta$ is given by

$$dQ_g = q(1 + \sin w\theta)d\theta \tag{10}$$

Since, at steady state, there is no net temperature change in the cylinder from one cycle to the next, an energy balance may be made in which

$$dQ_s + dQ_t = dQ_g \tag{11}$$

From Equations 4, 7, 10, and 11,

$$mCdT + hATd\theta = q(1 + \sin w\theta)d\theta$$

or

$$\frac{dT}{d\theta} + \frac{hA}{mC} T = \frac{q}{mC} (1 + \sin w\theta) \tag{12}$$

For convenience, let

$$\frac{hA}{mC} = C_1 \tag{13}$$

and

$$\frac{q}{mC} = C_2 \tag{14}$$

Equation 12 then becomes

$$\frac{dT}{d\theta} + C_1 T = C_2(1 + \sin w\theta) \tag{15}$$

If Equation 15 is multiplied through by $e^{C_1\theta}$,

$$e^{C_1\theta} \frac{dT}{d\theta} + C_1 T e^{C_1\theta} = C_2(1 + \sin w\theta)e^{C_1\theta} \tag{16}$$

The left side of Equation 16 is seen to be a perfect differential so that

$$Te^{C_1\theta} = \int C_2(1 + \sin w\theta)e^{C_1\theta} d\theta \tag{17}$$

or

$$Te^{C_1\theta} = C_2\left(\frac{1}{C_1}e^{C_1\theta} + \int e^{C_1\theta} \sin w\theta d\theta\right) \tag{18}$$

The remaining integration may be performed using standard integral tables and Equation 18 becomes, after simplification,

$$T = C_2\left(\frac{1}{C_1} + \frac{C_1 \sin w\theta - w \cos w\theta}{C_1^2 + w^2} + \frac{C_3}{e^{C_1\theta}}\right) \tag{19}$$

where C_3 is the constant of integration.

Since

$$\frac{C_2}{C_1} = \frac{q}{hA}$$

and by definition of h,

$$h = \frac{q}{AT_a} \tag{20}$$

in which both q and T_a are average quantities, used in calculating h, Equation 19 simplifies to

$$T - T_a = C_2 \left(\frac{C_1 \sin w\theta - w \cos w\theta}{C_1^2 + w^2} + C_3 e^{-C_1\theta}\right) \tag{21}$$

Also because of Equation 20, the instantaneous temperature difference, T, and the instantaneous heat generation rate, q_i, are in phase. In view of this, the boundary conditions for the problem are

(a) $w\theta = 0$

$T = T_a$

and

(b) $w\theta = \frac{\pi}{2}$

$T = T_m$

where T_m is the maximum temperature difference at the instant of maximum heat generation rate. By using boundary condition a,

$$C_3 = \frac{w}{C_1^2 + w^2} \tag{22}$$

The amplitude, a_o, of the temperature difference fluctuation is stated by

$$a_o = T_m - T_a \tag{23}$$

Applying Equation 22 and boundary condition b to Equation 21 yields, after substitution of Equation 23,

$$a_o = \frac{C_2}{C_1^2 + w^2} \left(C_1 + we^{\frac{-C_1\pi}{2w}}\right) \tag{24}$$

Equation 24 may be simplified for the special case of the metal cylinder being a thin metal film. In this case

$$\frac{C_1}{w} >> 1$$

and the term $we^{\frac{-C_1\pi}{2w}}$ becomes negligible compared with C_1. For a heat transfer coefficient as small as 100, for the gold films used, C_1 is on the order of 10^7 and the term $we^{\frac{-C_1\pi}{2w}}$ is on the order of 10^4. Equation 24 then becomes

$$a_o = \frac{C_1C_2}{C_1^2 + w^2} \tag{25}$$

or

$$a_o = \frac{C_2}{C_1} \frac{1}{1 + \left(\frac{w}{C_1}\right)^2} \tag{26}$$

and since

$$\frac{w}{C_1} << 1$$

Equation 26 becomes

$$a_o = \frac{C_2}{C_1} \tag{27}$$

Substituting Equation 13, 14, and 20,

$$a_o = T_a \tag{28}$$

Interpreting this result, one sees that, during the AC heating of the film, the film temperature fluctuates between the temperature of the environment and a value double its average level. This extreme temperature cycling would undoubtedly affect the mechanical properties of the film. Since the mechanical properties of thin films are known to deviate radically from those of the bulk metal, no intelligent evaluation may be made of the possibility of strain hardening in the film and the consequent effects on the electrical resistance, at least without considerable extension of the experimental program followed.

Since the heat capacity of the films was exceedingly small and the response time was short, the burnout of the film would follow a different pattern from that of a thicker metal cylinder. As the sinusoidal power is built from the average value, the temperature of the film will follow. If, at the peak of the power curve, the film can transfer all

the heat being generated, burnout will not occur. If, on the other hand, the surface of the film becomes vapor bound at the peak of the curve, the film will immediately be heated to its melting point and be burned out. At the burnout of the film, then, it is actually transferring double the average electrical power indicated on the monitoring meters and, within the limits of the assumptions made in the previous derivation, is at double the average temperature indicated by the average resistance of the film. For this reason, the burnout flux recorded in this investigation was taken as double the value indicated on the meters at the time of burnout.

The results of the experimental runs showed assumptions c and d in the previous investigation to be incorrect. A better approach may be made based on the observation, from the data taken, that the heat transfer rate is an exponential function of surface temperature. Substituting the following assumptions for assumptions c and d allows a more accurate derivation to be carried out:

(a) Heat flux at the film surface, q_t, is an exponential function of temperature difference

(b) Electrical resistance of the film is a linear function of temperature difference.

From assumption a,

$$q_t = C_1 T^{C_2} \tag{29}$$

and

$$dQ_t = C_1 T^{C_2}\, d\theta \tag{30}$$

From assumption b, the resistance of the film is stated by

$$R = C_3 + C_4 T \tag{31}$$

The heat generation rate is then

$$q_g = \frac{3.41\ E^2_m \sin^2 w\theta}{C_3 + C_4 T} \tag{32}$$

where E_m is the peak voltage generated and

$$w = 2\pi f \tag{33}$$

in which f represents the frequency of the voltage variation, 216,000 cycles per hour for 60 cycle AC. θ is the time defined so that the instantaneous voltage equals zero at time zero. Under these conditions, the temperature difference T equals zero at time zero. In terms of the average voltage, E, which would be read from a voltmeter, since

$$E = \sqrt{2}\, E_m$$

Equation 32 becomes

$$q_g = \frac{6.82\ E^2 \sin^2 w\theta}{C_3 + C_4T} \tag{34}$$

and the heat generated in the time interval $d\theta$ becomes

$$dQ_g = \frac{6.82\ E^2 \sin^2 w\theta}{C_3 + C_4T}\, d\theta \tag{35}$$

Under these new conditions Equation 12 becomes

$$\frac{dT}{d\theta} = \frac{6.82\ E^2 \sin^2 w\theta}{(C_3 + C_4T)\ mC} - \frac{C_1T^{C_2}}{mC} \tag{36}$$

Equation 36 is seen to be a non-linear ordinary differential equation which cannot be solved in simple terms. The equation, however, is amenable to solution by the Runge-Kutta method of numerical approximation for which computer programs, using the Bell General Purpose System, are available.

For the case of the thin film, since the mass of the film is negligible, Equation 7 is negligible and Equations 29 and 35 may be equated to produce

$$6.82\ E^2 \sin^2 w\theta = (C_3 + C_4T)C_1T^{C_2} \tag{37}$$

Equation 37 may be solved by trial and error to determine the maximum temperature difference for a given impressed

voltage once the values of the constants are calculated, by noticing that, at the peak in the curve,

$$w\theta = \frac{\pi}{2}$$

Equation 37 then becomes, for the maximum temperature difference T_m,

$$6.82\ E^2 = (C_3 + C_4 T_m)\ C_1 T_m^{C_2} \qquad (38)$$

For run No. 19, which gave the highest burnout flux, the procedure of doubling the indicated flux at burnout and extrapolating the curve to this value to determine the burnout temperature gave values of $3,600,000\ \frac{Btu}{ft^2 hr}$ and $1520^{\circ}F$. Solution of Equation 38 for this case gave $3,400,000\ \frac{Btu}{ft^2 hr}$ and $1590^{\circ}F$. In view of this close agreement and the tedious calculations required for the solution of Equation 38, the doubling technique was used for all burnout values.

Since the outer surface of the Pyrex spacers did no more than grow warm to the touch during the runs, no corrections were applied for heat loss through the spacer. An analysis was made, however, of the axial temperature distribution in the film to allow conduction losses to the brass electrodes to be estimated. The following assumptions were made:

(a) Temperatures of the electrodes constant and equal to the environment temperature

(b) Constant heat transfer coefficient from the film surface

(c) No radial temperature gradient

(d) Perfectly insulated exterior film surface

(e) Uniform volumetric heat generation in the film

(f) Steady state

By the Fourier Equation, $(q_C)_i$, the heat conducted into a differential element of the cylindrical film is

$$(q_C)_i = -kA_C(\frac{dt}{dx})x \tag{39}$$

where k is the thermal conductivity, A_C is the cross sectional area of the film, and $(\frac{dt}{dx})_x$ is the temperature gradient at some axial distance, x, from the midpoint of the cylinder. In the same manner $(q_C)_o$, the heat conducted out is

$$(q_C)_o = kA_C(\frac{dt}{dx})x + dx \tag{40}$$

where $(\frac{dt}{dx})x + dx$ is the temperature gradient at some axial distance, $x + dx$, from the midpoint of the cylindrical film. The heat, q_b, convected from the surface of the differential film element is given by

$$q_b = h\ (t - t_e)\ dA_s \tag{41}$$

in which h is the heat transfer coefficient, t is the film temperature, t_e is the environment temperature, and dA_s is the surface area of the differential film element. Since

$$dA_s = \pi D dx \tag{42}$$

where D is the diameter of the film cylinder, Equation 31 becomes

$$q_b = \pi D h (t - t_e) dx \tag{43}$$

The heat generated, q_g, in the differential element is given by

$$q_g = q''' A_c dx \tag{44}$$

in which q''' is the volumetric heat generation rate. Under assumption f, an energy balance may be made. Combining Equations 39, 40, 43, and 44, this balance becomes

$$-kA_c \left(\frac{dt}{dx}\right)_x + q''' A_c dx = -kA_c \left(\frac{dt}{dx}\right)_{x+dx} + \pi D h (t - t_e) dx \tag{45}$$

Grouping the conduction terms, dividing through by dx and allowing dx to approach zero reduces Equation 45 to

$$kA_c \frac{d^2t}{dx^2} + q''' A_c = \pi D h (t - t_e) \tag{46}$$

Treatment of Equation 46 is facilitated by making the substitutions

$$T = t - t_e \tag{47}$$

and

$$d^2T = d^2t \tag{48}$$

so that Equation 46 becomes

$$dA_C \frac{d^2T}{dx^2} + q'''A_C = \pi DhT \tag{49}$$

Simplifying and substituting

$$C_1 = \frac{q'''}{k} \tag{50}$$

and

$$C_2 = \frac{\pi Dh}{kA_C} \tag{51}$$

Equation 49 is reduced to

$$\frac{d^2T}{dx^2} - C_1T = -C_2 \tag{52}$$

The left side of Equation 52 is a homogeneous linear differential equation of second order, the solution of which leads to the complimentary solution,

$$T_C = C_3e^{\sqrt{C_2}x} + C_4e^{-\sqrt{C_2}x} \tag{53}$$

A particular solution of Equation 53 is found, by Lagrange's method of variation of parameters, to be

$$T_p = \frac{C_1}{C_2} \tag{54}$$

Adding the complimentary and particular solutions gives the *general solution for Equation 52*

$$T = C_1 e^{\sqrt{C_2}x} + C_2 e^{-\sqrt{C_2}x} + \frac{C_1}{C_2} \tag{55}$$

The boundary conditions for this case are

$$\text{(a)} \quad \frac{dT}{dx} = 0$$

$$x = 0$$

$$\text{(b)} \quad T = 0$$

$$x = L$$

where L is the axial distance from the midpoint of the cylindrical film to the electrode. Application of these boundary conditions to Equation 55 produces the result,

$$T = \frac{C_1}{C_2}\left(1 - \frac{e^{\sqrt{C_2}x} + e^{-\sqrt{C_2}x}}{e^{\sqrt{C_2}L} + e^{-\sqrt{C_2}L}}\right) \tag{56}$$

The first derivative of Equation 56, evaluated at $x = L$, gives the temperature gradient in the film at the electrode.

$$\left(\frac{dT}{dx}\right)_L = -\frac{C_1}{C_2}\left(\frac{e^{\sqrt{C_2}L} - e^{-\sqrt{C_2}L}}{e^{\sqrt{C_2}L} + e^{-\sqrt{C_2}L}}\right) \tag{57}$$

Recalling that, from Equation 51,

$$C_2 = \frac{\pi Dh}{kA_C}$$

the small cross sectional area of the film, about 10^{-7} ft^2, causes the terms $e^{-\sqrt{C_2}L}$ to be negligible. Equation 57 then reduces to

$$\left(\frac{dT}{dx}\right)_L = \frac{-C_1}{\sqrt{C_2}} \tag{58}$$

and q_C, the loss by conduction to the electrode, is given by Fourier's Equation as

$$q_C = kA_C \frac{C_1}{\sqrt{C_2}} \tag{59}$$

The volumetric heat generation rate is given by

$$q''' = \frac{q}{2LA_C} \tag{60}$$

where q is the heat generation rate in the film as a whole. Since the film is very thin,

$$A_C = \pi Ds \tag{61}$$

where s represents the thickness of the film. Combining Equations 50, 51, 59, 60, and 61, and simplifying gives

$$\frac{q_C}{q} = \frac{1}{2L}\sqrt{\frac{ks}{h}} \qquad (62)$$

Since the thickness of the film is negligible compared to the heat transfer coefficient, Equation 62 reduces to zero and no correction for conduction loss is necessary.

CHAPTER V

CONCLUSIONS AND RECOMMENDATIONS

The conclusions reached in this study may be stated as follows:

1. The use of thin gold films as resistance heaters in heat transfer experiments employing low current, high voltage power is feasible.

2. Since the thin films have extremely rapid response, the choice of adequate instrumentation is limited to recording oscillographs or tape recorders.

3. The heat fluxes obtainable in low velocity swirling flow are due not to high heat transfer coefficients, but to high permissible operating temperatures.

4. The burnout heat fluxes depend on the tangential velocity and were found to range, for the velocities used, from 1,420,000 to 3,600,000 Btu/ft^{2}hr.

5. Reasons were observed for stating that the mechanism of heat transfer in the swirling flow in contact with hot metal walls was probably forced convection, not boiling.

From the results of this investigation, several avenues of further work became apparent. Foremost among these is the concrete determination of the mechanism of swirling

heat transfer, whether by boiling or by forced convection under high gravitational fields. One approach, through the use of thin film heating elements, would be the elimination of optical interference from the free water surface and the visual observation of wall phenomena through the films.

A second interesting investigation would be the use of higher temperature films, such as platinum, to ascertain whether the film surface actually becomes vapor blanketed at the heat fluxes used or the gold films merely melted because of high operating temperatures.

A study should be made to determine the effect of tangential flow on the critical temperature drop at burnout. Determinations should be made with linear flow first, then extended to mild swirling, induced by twisted wires and strips, and finally to strong swirling in a system similar to that used in this investigation. The effect of the degree of water subcooling should be included in this study.

Since the films were seen to respond rapidly to changes in the power generation rates, they could be used in transient convection or boiling to determine the behavior of the fluid boundary. High speed instrumentation would obviously be necessary for such a study.

APPENDIX I

EXPERIMENTAL AND CALCULATED DATA

Table 3. Data for Run No. 2

Impeller Number B-38

Inlet Pressure: 37 psig
Flow Rate: 6.53 gpm
Total Velocity: 45.1 fps
Inlet Water Temperature: 70°F
Film Length: 1.38 in.

Voltage (volts)	Current (amps)	Power (kw)	Heat Flux ($\frac{Btu}{hr\ ft^2}$)	Resistance (ohms)	Film Temp. (°F)	Temp. Difference (°F)
9.1	45.6	0.416	47,500	0.199	595	525
12.6	60.4	0.761	86,800	0.209	685	615
16.9	74.0	1.25	143,000	0.228	850	780
20.9	88.9	1.86	212,000	0.235	910	840
22.2	105	2.33	266,000	0.211	725	655
32.4	128	4.15	473,000	0.253	1035	965
34.9	125	4.36	497,000	0.279	1180	1110
44.9	146	6.55	746,000	0.307	1340	1270
49.1	164	8.06	920,000	0.300	1290	1220
59.0	180	10.6	1,210,000	0.328	1450	1380

Table 4. Data for Run No. 4

Impeller Number B-14

Inlet Pressure: 16 psig
Flow Rate: 3.2 gpm
Total Velocity: 33 fps
Inlet Water Temperature: 70°F
Film Length: 1.38 in.

Voltage (volts)	Current (amps)	Power (kw)	Heat Flux ($\frac{Btu}{hr\ ft^2}$)	Resistance (ohms)	Film Temp. (°F)	Temp. Difference (°F)
9.4	63.2	0.594	67,600	0.149	465	395
11.9	73.6	0.875	99,600	0.161	610	540
13.7	81.2	1.11	127,000	0.169	705	635
15.2	84.9	1.29	147,000	0.179	795	725
17.5	96.9	1.69	193,000	0.181	810	740
19.7	108	2.13	243,000	0.182	825	755
21.8	112	2.44	278,000	0.195	960	890
22.7	121	2.75	314,000	0.188	895	825
26.3	133	3.5	399,000	0.198	975	905
29.8	138	4.11	469,000	0.216	1110	1040
30.6	158	4.84	551,000	0.194	935	865
35.5	160	5.68	648,000	0.222	1160	1090
38.2	167	6.38	727,000	0.229	1210	1140
39.1	177	6.92	789,000	0.222	1160	1090
48.1	186	8.95	1,020,000	0.259	1400	1333

Table 5. Data for Run No. 7

Impeller Number B-38

Inlet Pressure: 22 psig
Flow Rate: 5.0 gpm
Total Velocity: 34.4 fps
Inlet Water Temperature: 70°F
Film Length: 1.38 in.

Voltage (volts)	Current (amps)	Power (kw)	Heat Flux ($\frac{Btu}{hr\ ft^2}$)	Resistance (ohms)	Film Temp. (°F)	Temp. Difference (°F)
8.9	50.4	0.449	51,100	0.177	520	450
11.3	59.2	0.669	76,100	0.191	650	580
12.5	64.9	0.810	92,300	0.193	665	595
14.3	72.0	1.03	117,000	0.199	725	655
16.8	82.9	1.39	158,000	0.203	760	690
19.9	93.2	1.86	212,000	0.215	865	795
22.2	103	2.29	261,000	0.216	870	800
24.9	115	2.86	326,000	0.217	875	805
28.2	116	3.27	373,000	0.233	1075	1005
32.7	139	4.55	519,000	0.236	1025	955
39.4	150	5.91	675,000	0.263	1190	1120
41.1	159	6.54	745,000	0.259	1170	1100
59.1	153	9.05	1,030,000	0.386	1260	1190

Table 6. Data for Run No. 9

Impeller Number B-14

Inlet Pressure: 4 psig
Flow Rate: 1.91 gpm
Total Velocity: 19.6 fps
Inlet Water Temperature: 70°F
Film Length: 1.38 in.

Voltage (volts)	Current (amps)	Power (kw)	Heat Flux ($\frac{Btu}{hr\ ft^2}$)	Resistance (ohms)	Film Temp. (°F)	Temp. Difference (°F)
8.4	42.9	0.360	41,000	0.196	415	345
11.4	50.9	0.580	66,100	0.224	575	505
13.8	55.2	0.762	87,000	0.250	770	700
17.7	71.2	1.26	144,000	0.249	755	685
20.7	84.0	1.74	199,000	0.246	735	665
29.7	114	3.38	385,000	0.261	845	775
32.1	110	3.53	402,000	0.292	1030	960
34.4	121	4.16	475,000	0.284	995	925
38.5	132	5.08	579,000	0.292	1040	975
42.6	146	6.22	710,000	0.292	1040	965

Table 7. Data for Run No. 10

Impeller Number B-14

Inlet Pressure: 69 psig
Flow Rate: 6.43 gpm
Total Velocity: 66.2 fps
Inlet Water Temperature: 70°F
Film Length: 1.38 in.

Voltage (volts)	Current (amps)	Power (kw)	Heat Flux ($\frac{Btu}{hr\ ft^2}$)	Resistance (ohms)	Film Temp. (°F)	Temp. Difference (°F)
10.1	47.2	0.477	54,400	0.214	435	365
12.2	54.0	0.659	75,000	0.226	510	440
14.6	57.6	0.843	96,000	0.253	710	640
18.3	73.2	1.34	153,000	0.250	695	625
22.3	84.5	1.88	214,000	0.264	795	725
24.4	92.9	2.27	259,000	0.263	785	715
34.4	116	3.99	455,000	0.297	975	905
37.3	131	4.89	557,000	0.285	925	855
43.1	142	6.14	700,000	0.304	1035	965
49.2	150	7.39	842,000	0.328	1150	1080
54.6	166	9.08	1,040,000	0.329	1160	1090
60.6	171	10.4	1,190,000	0.355	1280	1210
69.3	195	13.5	1,540,000	0.355	1280	1210

Table 8. Data for Run No. 13

Impeller Number B-38

Inlet Pressure: 7 psig
Flow Rate: 2.98 gpm
Total Velocity: 20.7 fps
Inlet Water Temperature: 70°F
Film Length: 1.38 in.

Voltage (volts)	Current (amps)	Power (kw)	Heat Flux ($\frac{Btu}{hr\ ft^2}$)	Resistance (ohms)	Film Temp. (°F)	Temp. Difference (°F)
7.1	29.2	0.207	23,600	0.243	535	465
9.7	36.4	0.353	40,200	0.266	685	615
10.9	40.8	0.445	50,700	0.268	715	645
13.0	48.8	0.634	72,200	0.267	700	630
15.9	53.6	0.852	97,100	0.296	885	815
17.2	52.4	0.901	103,000	0.328	1050	980
20.9	64.5	1.35	154,000	0.324	1035	965
25.9	76.5	1.98	226,000	0.338	1090	1020
29.6	83.2	2.46	280,000	0.356	1180	1110
37.3	100.	3.73	425,000	0.373	1250	1180
41.9	99.3	4.15	473,000	0.422	1460	1390
48.1	109	5.25	599,000	0.442	1550	1480
57.2	116	6.65	759,000	0.493	1780	1710

Table 9. Data for Run No. 14

Impeller Number B-12

Inlet Pressure: 21 psig
Flow Rate: 7.45 gpm
Total Velocity: 38.2 fps
Inlet Water Temperature: 70°F
Film Length: 1.38 in.

Voltage (volts)	Current (amps)	Power (kw)	Heat Flux ($\frac{Btu}{hr\ ft^2}$)	Resistance (ohms)	Film Temp. (°F)	Temp. Difference (°F)
9.2	51.6	0.475	54,100	0.178	575	505
12.9	65.6	0.846	96,500	0.197	765	695
15.8	76.9	1.21	138,000	0.206	840	770
16.6	80.9	1.34	153,000	0.205	815	745
22.6	105	2.37	270,000	0.215	915	845
26.4	118	3.11	355,000	0.224	970	900
31.6	129	4.07	464,000	0.245	1120	1050
34.2	128	4.38	499,000	0.267	1260	1190
39.2	144	5.65	645,000	0.272	1290	1220
47.3	167	7.89	899,000	0.283	1350	1280
55.4	176	9.75	1,110,000	0.315	1560	1490

Table 10. Data for Run No. 15

Impeller Number B-14

Inlet Pressure: 41 psig
Flow Rate: 4.75 gpm
Total Velocity: 49.1 fps
Inlet Water Temperature: 70°F
Film Length: 1.38 in.

Voltage (volts)	Current (amps)	Power (kw)	Heat Flux ($\frac{Btu}{hr\ ft^2}$)	Resistance (ohms)	Film Temp. (°F)	Temp. Difference (°F)
5.2	39.2	0.204	23,200	0.132	495	425
6.85	48.9	0.335	38,200	0.140	615	545
7.9	56.0	0.442	50,400	0.141	640	570
9.6	65.2	0.627	71,500	0.147	705	635
10.5	66.9	0.702	80,000	0.157	810	740
13.1	82.5	1.08	123,000	0.159	835	765
15.5	95.6	1.48	169,000	0.163	885	815
22.1	130	2.87	327,000	0.170	955	885
23.8	126	3.0	342,000	0.189	1120	1050
26.6	140	3.73	425,000	0.190	1130	1060
32.4	136	4.4	501,000	0.238	1510	1440
34.6	165	5.7	650,000	0.210	1300	1230
37.8	171	6.46	738,000	0.221	1380	1310
46.1	196	9.05	1,030,000	0.236	1490	1420
51.2	225	11.5	1,310,000	0.228	1430	1360

Table 11. Data for Run No. 18

Impeller Number B-18

Inlet Pressure: 35 psig
Flow Rate: 2.38 gpm
Total Velocity: 49.2 fps
Inlet Water Temperature: 70°F
Film Length: 1.38 in.

Voltage (volts)	Current (amps)	Power (kw)	Heat Flux ($\frac{Btu}{hr\ ft^2}$)	Resistance (ohms)	Film Temp. (°F)	Temp. Difference (°F)
9.2	50.4	0.464	52,900	0.183	530	460
10.8	55.3	0.597	68,000	0.196	645	575
12.4	61.2	0.759	86,400	0.203	715	645
13.6	64.5	0.877	100,000	0.211	795	725
16.5	76.5	1.26	144,000	0.216	835	765
19.5	103	2.01	229,000	0.200	692	622
24.2	109	2.64	301,000	0.221	887	817
27.5	114	3.14	358,000	0.241	1025	955
32.8	131	4.3	490,000	0.251	1090	1020
34.1	130	4.43	505,000	0.262	1160	1090
39.8	144	5.74	654,000	0.276	1240	1170
45.1	157	7.1	809,000	0.288	1300	1230
51.7	173	8.95	1,020,000	0.299	1360	1290
56.6	174	9.54	1,120,000	0.326	1510	1440

Table 12. Data for Run No. 19

Impeller Number B-18

Inlet Pressure: 98 psig
Flow Rate: 3.90 gpm
Total Velocity: 80.2 fps
Inlet Water Temperature: 70°F
Film Length: 1.38 in.

Voltage (volts)	Current (amps)	Power (kw)	Heat Flux ($\frac{Btu}{hr\ ft^2}$)	Resistance (ohms)	Film Temp. (°F)	Temp. Difference (°F)
13.2	50.9	0.671	76,500	0.260	628	558
16.5	64.5	1.07	121,000	0.256	620	550
19.8	71.6	1.42	162,000	0.276	735	665
23.8	83.3	1.99	226,000	0.286	775	705
28.4	95.3	2.71	309,000	0.298	855	785
34.5	106	3.65	416,000	0.326	1020	950
41.7	125	5.21	595,000	0.333	1055	985
46.4	137	6.35	724,000	0.338	1090	1020
58.9	165	9.7	1,100,000	0.357	1170	1100
80.4	197	15.8	1,800,000	0.408	1380	1310

Table 13. Data for Run No. 21

Impeller Number B-18

Inlet Pressure: 14 psig
Flow Rate: 1.56 gpm
Total Velocity: 32.1 fps
Inlet Water Temperature: 70°F
Film Length: 1.38 in.

Voltage (volts)	Current (amps)	Power (kw)	Heat Flux ($\frac{Btu}{hr\ ft^2}$)	Resistance (ohms)	Film Temp. (°F)	Temp. Difference (°F)
7.29	40.9	0.297	33,900	0.179	445	375
8.61	45.2	0.390	44,500	0.191	525	455
9.92	46.9	0.465	53,000	0.212	715	645
11.9	56.5	0.672	76,600	0.211	705	635
15.0	68.0	1.02	116,000	0.221	780	710
15.6	67.3	1.05	120,000	0.232	865	795
17.2	74.5	1.28	146,000	0.231	870	800
20.9	87.3	1.83	209,000	0.240	925	855
24.8	107	2.66	303,000	0.232	865	795
31.3	113	3.54	404,000	0.277	1170	1100
35.1	114	4.0	456,000	0.308	1320	1250
43.1	138	5.95	679,000	0.313	1350	1280
48.6	151	7.35	838,000	0.322	1400	1330
59.4	163	9.67	1,100,000	0.364	1640	1570

Table 14. Data for Run No. 22

Impeller Number B-12

Inlet Pressure: 14 psig
Flow Rate: 5.0 gpm
Total Velocity: 25.7 fps
Inlet Water Temperature: 70°F
Film Length: 1.38 in.

Voltage (volts)	Current (amps)	Power (kw)	Heat Flux ($\frac{Btu}{hr\ ft^2}$)	Resistance (ohms)	Film Temp. (°F)	Temp. Difference (°F)
8.31	42.4	0.352	40,100	0.162	515	445
10.1	52.8	0.533	60,800	0.192	830	760
11.1	61.2	0.679	77,400	0.181	720	650
12.4	63.6	0.789	90,900	0.195	855	785
14.3	75.6	1.08	123,000	0.189	795	725
18.6	88.4	1.69	187,000	0.211	980	910
20.9	89.2	1.85	211,000	0.232	1160	1090
24.8	98.8	2.45	279,000	0.251	1260	1190
27.0	116	3.13	355,000	0.239	1150	1080
31.8	122	3.88	443,000	0.261	1320	1250
39.5	142	5.61	640,000	0.278	1430	1360
45.6	149	6.8	775,000	0.306	1590	1520
51.2	160	8.2	935,000	0.319	1680	1610

Table 15. Data for Burnout Runs

Inlet Water Temperature: 70°F
Film Length: 1.38 in.

Run Number	Impeller Number	Inlet Velocity ($\frac{ft}{sec}$)	Inlet Pressure (psig)	Voltage (volts)	Current (amps)	Power (kw)	Burnout Heat Flux ($\frac{Btu}{hr\ ft^2}$)
1	B-18	56.9	45	81.4	144	11.7	2,660,000
*3	B-12	37.8	29	66.0	134	8.87	2,020,000
*5	B-12	39.2	30	68.3	157	10.8	2,440,000
6	B-12	39.0	31	58.6	158	9.26	2,120,000
8	B-12	31.2	18	56.9	141	8.00	1,824,000
11	B-18	78.9	91	76.1	168	12.8	2,920,000
12	B-12	20.0	11	55.3	122	6.76	1,540,000
16	B-14	42.5	29	73.5	159	11.7	2,660,000
17	B-18	58.0	46	77.3	165	12.8	2,920,000
20	B-38	40.1	29	62.1	133	8.26	1,880,000
23	B-12	23.4	12	53.1	131	6.96	1,590,000
24	B-18	70.8	73	76.3	166	12.7	2,880,000
25	B-14	54.1	48	58.9	180	10.6	2,420,000
26	B-14	28.4	19	52.3	152	7.94	1,810,000

*-Water was degassed by boiling before use

APPENDIX II

HEAT FLUX CURVES

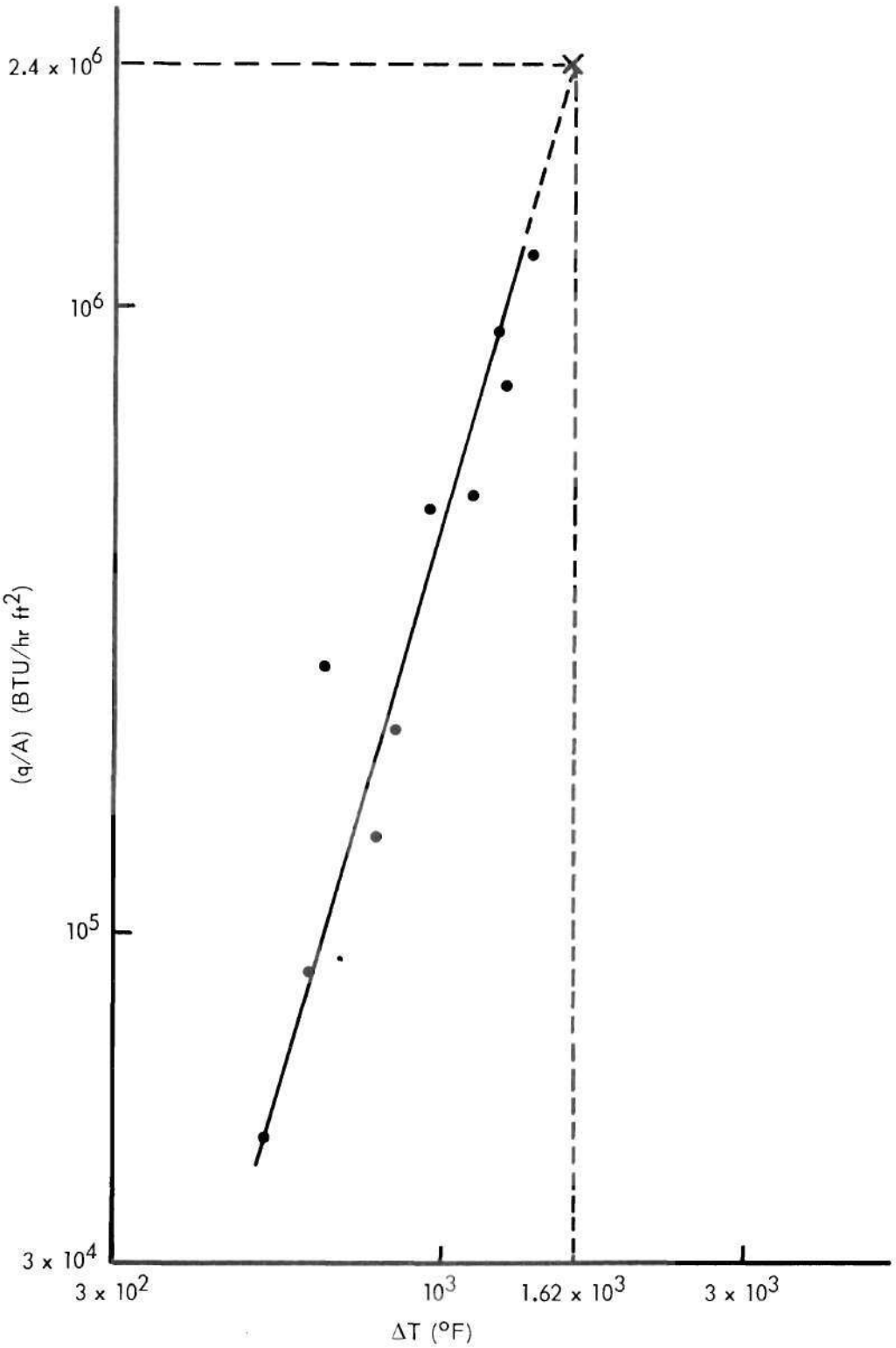

Figure 11. Heat Flux Curve for Run No. 2.

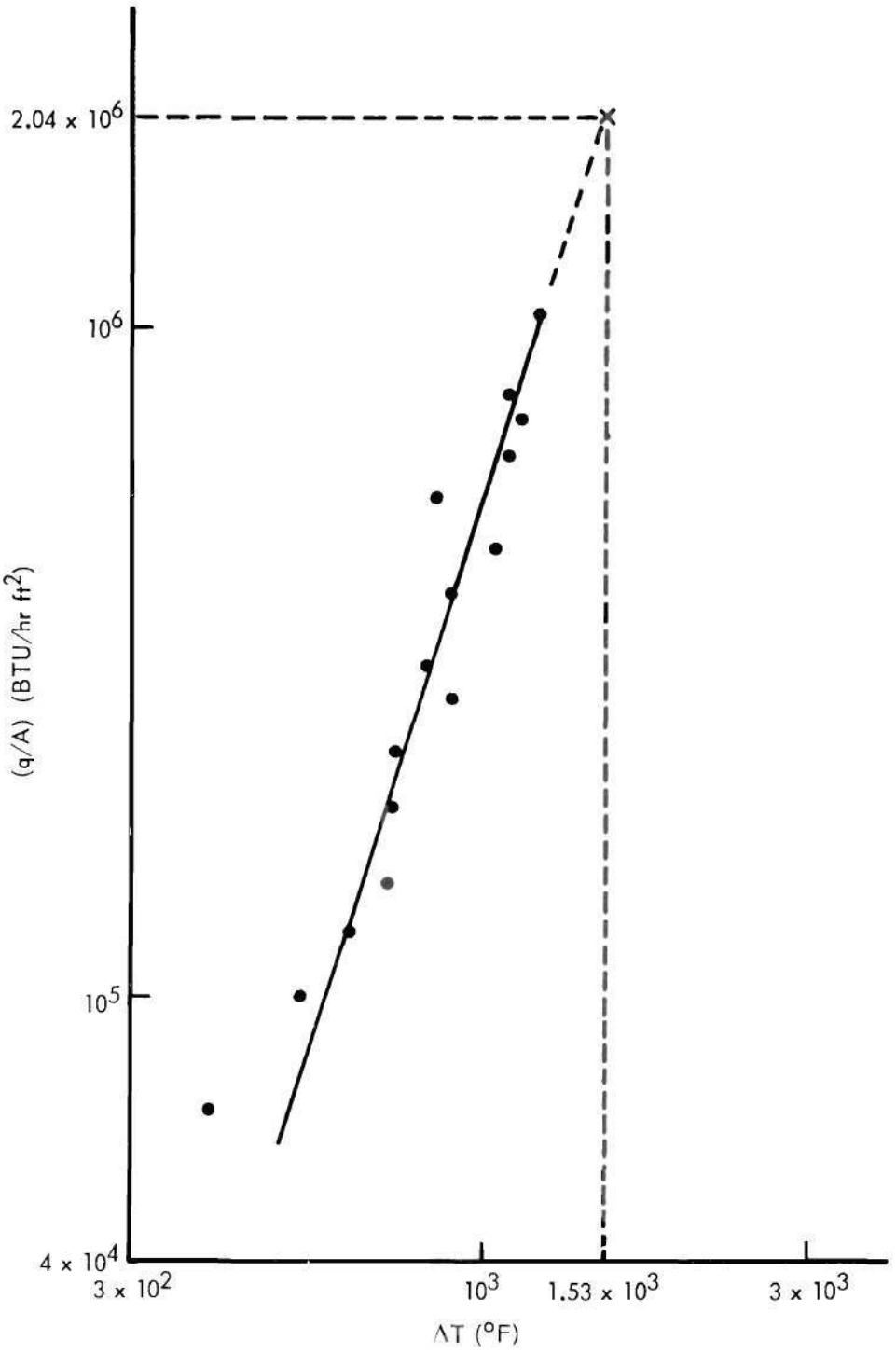

Figure 12. Heat Flux Curve for Run No. 4.

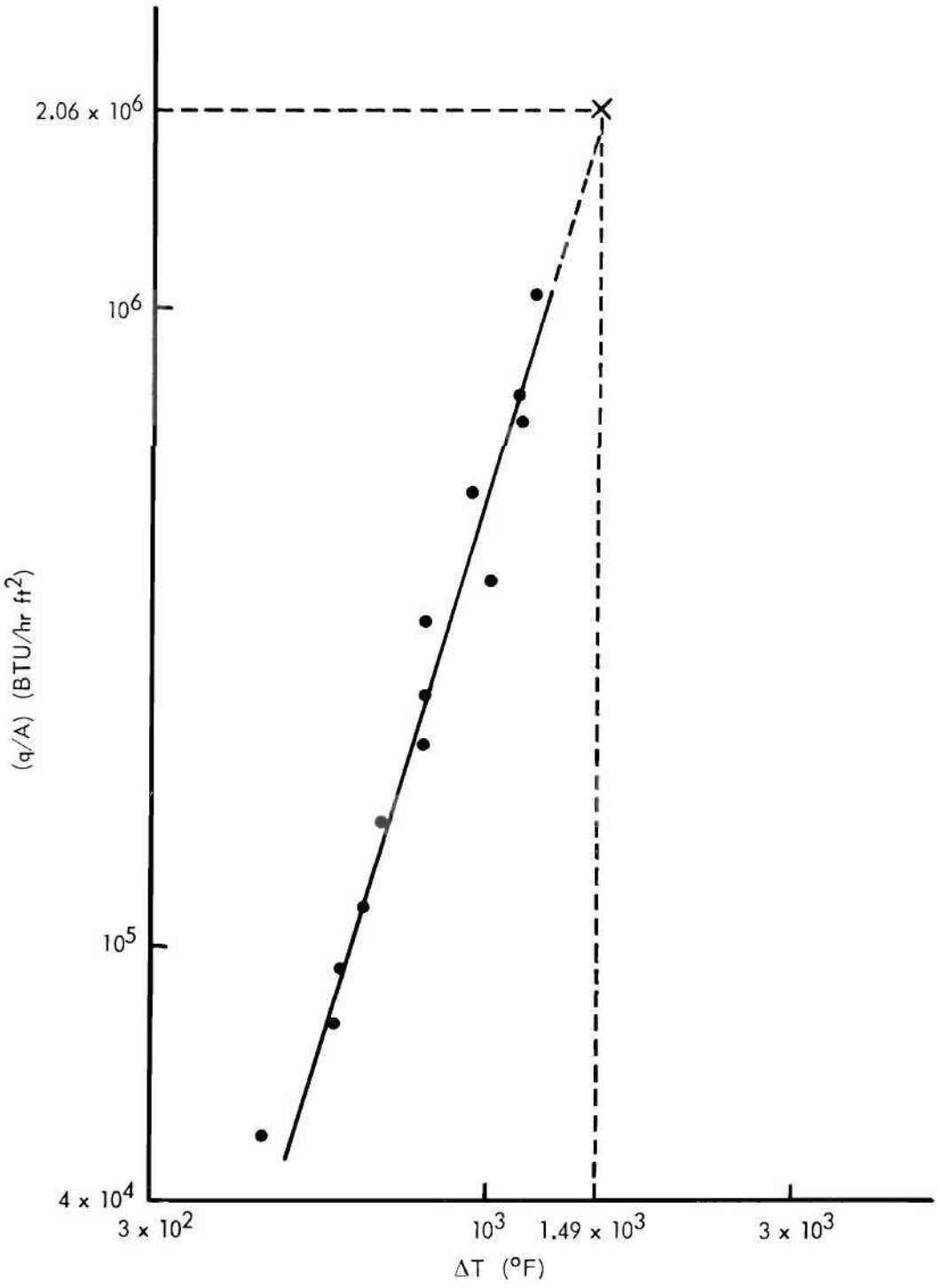

Figure 13. Heat Flux Curve for Run No. 7.

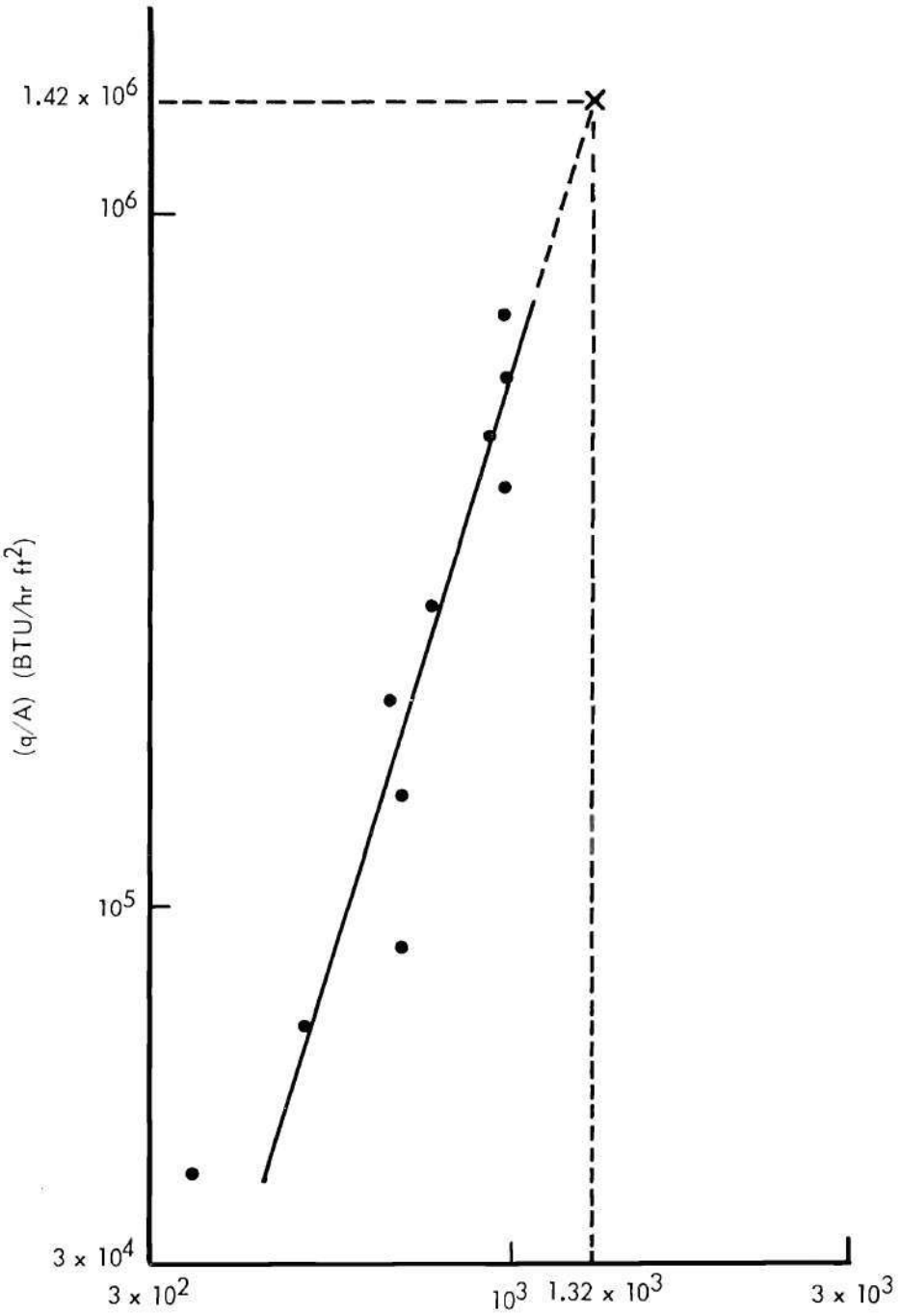

Figure 14. Heat Flux Curve for Run No. 9.

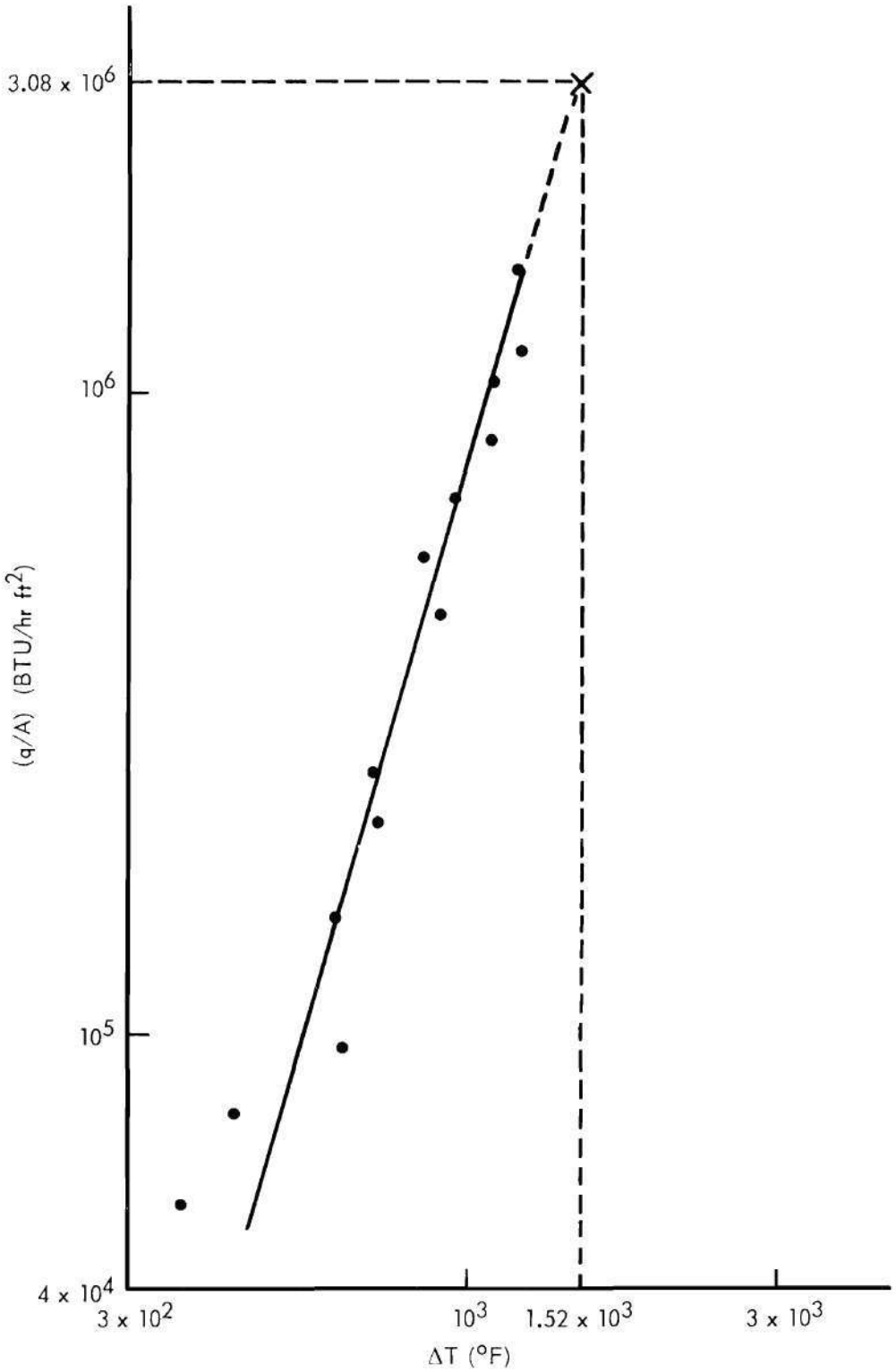

Figure 15. Heat Flux Curve for Run No. 10.

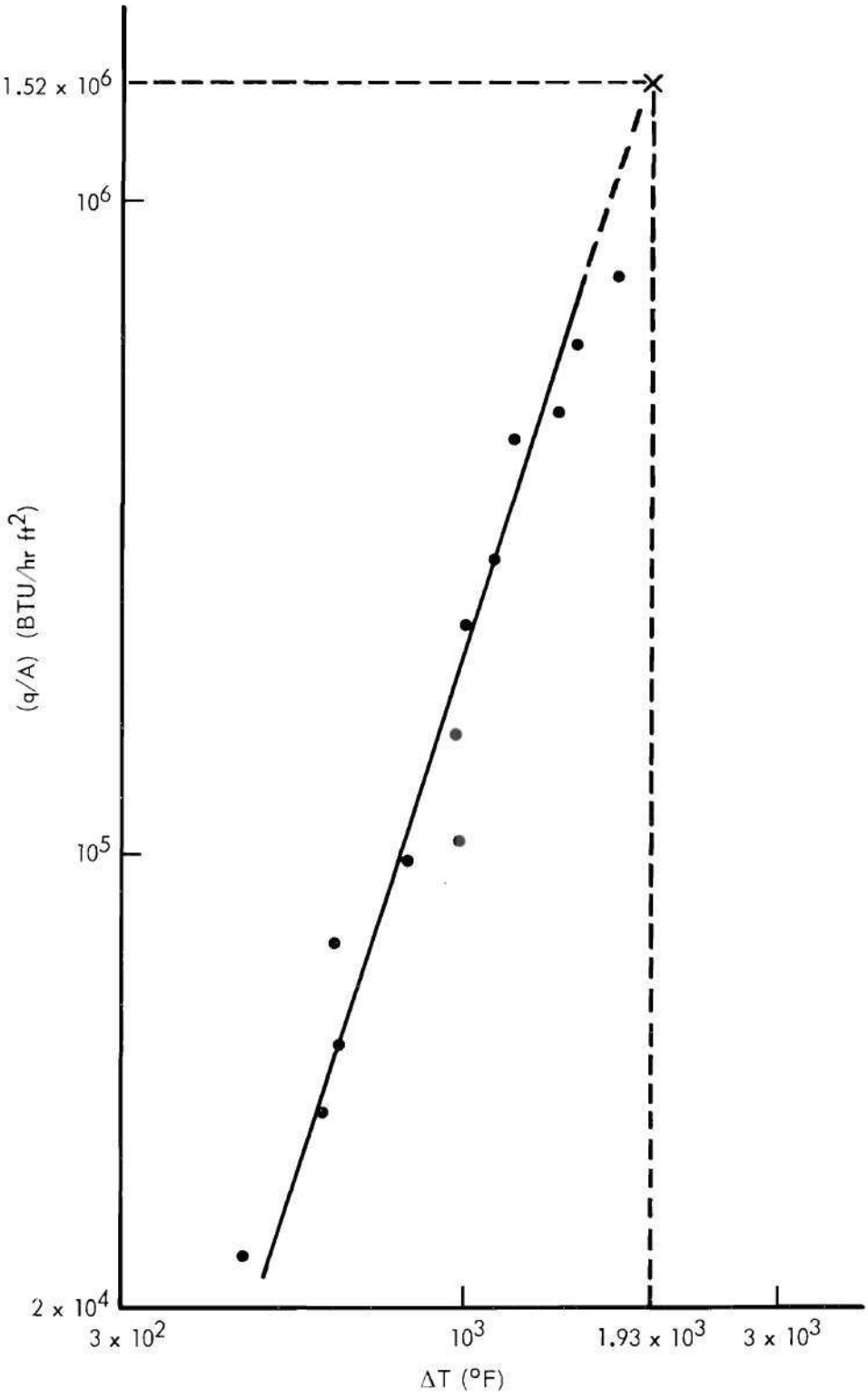

Figure 16. Heat Flux Curve for Run No. 13.

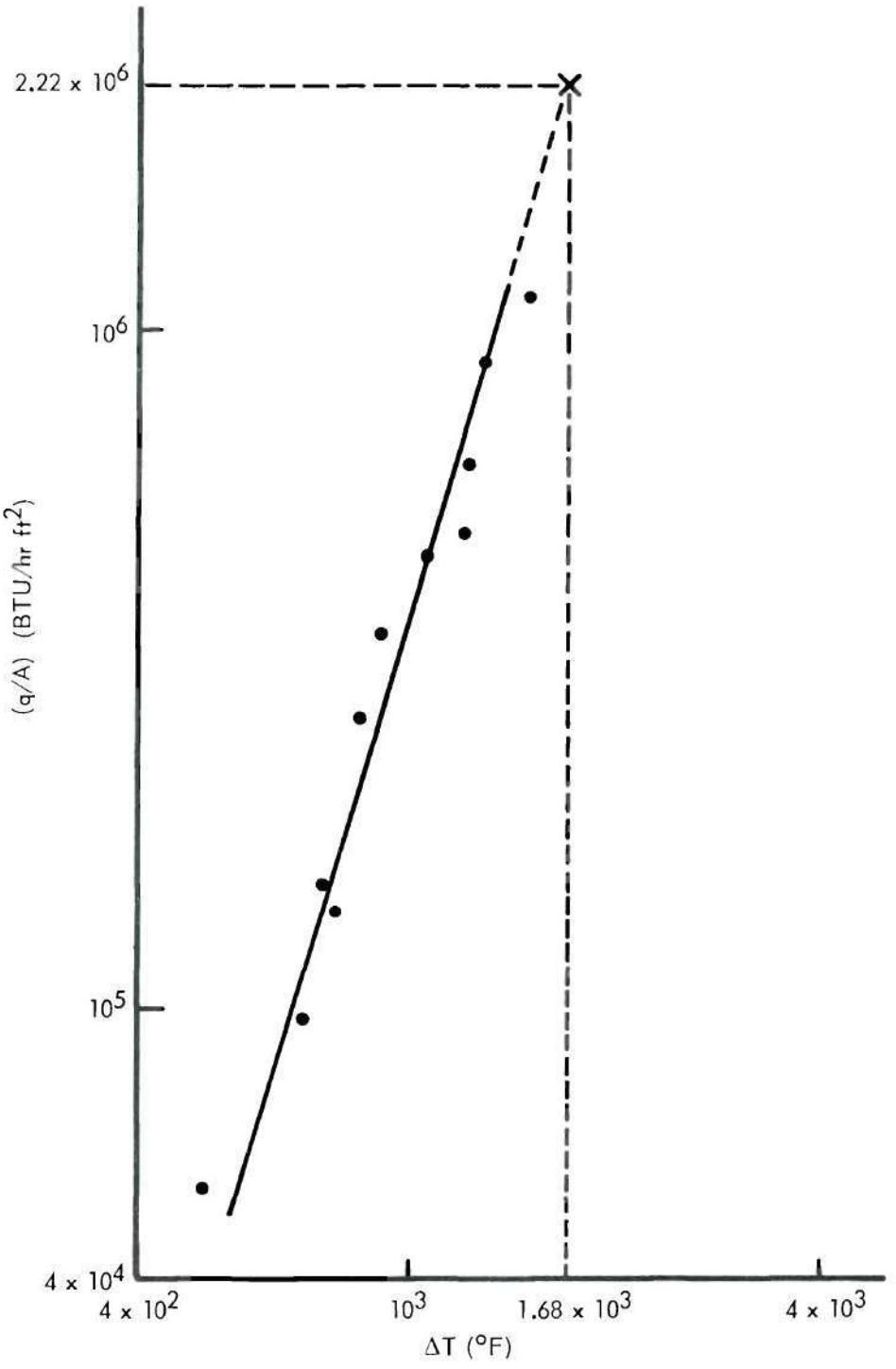

Figure 17. Heat Flux Curve for Run No. 14.

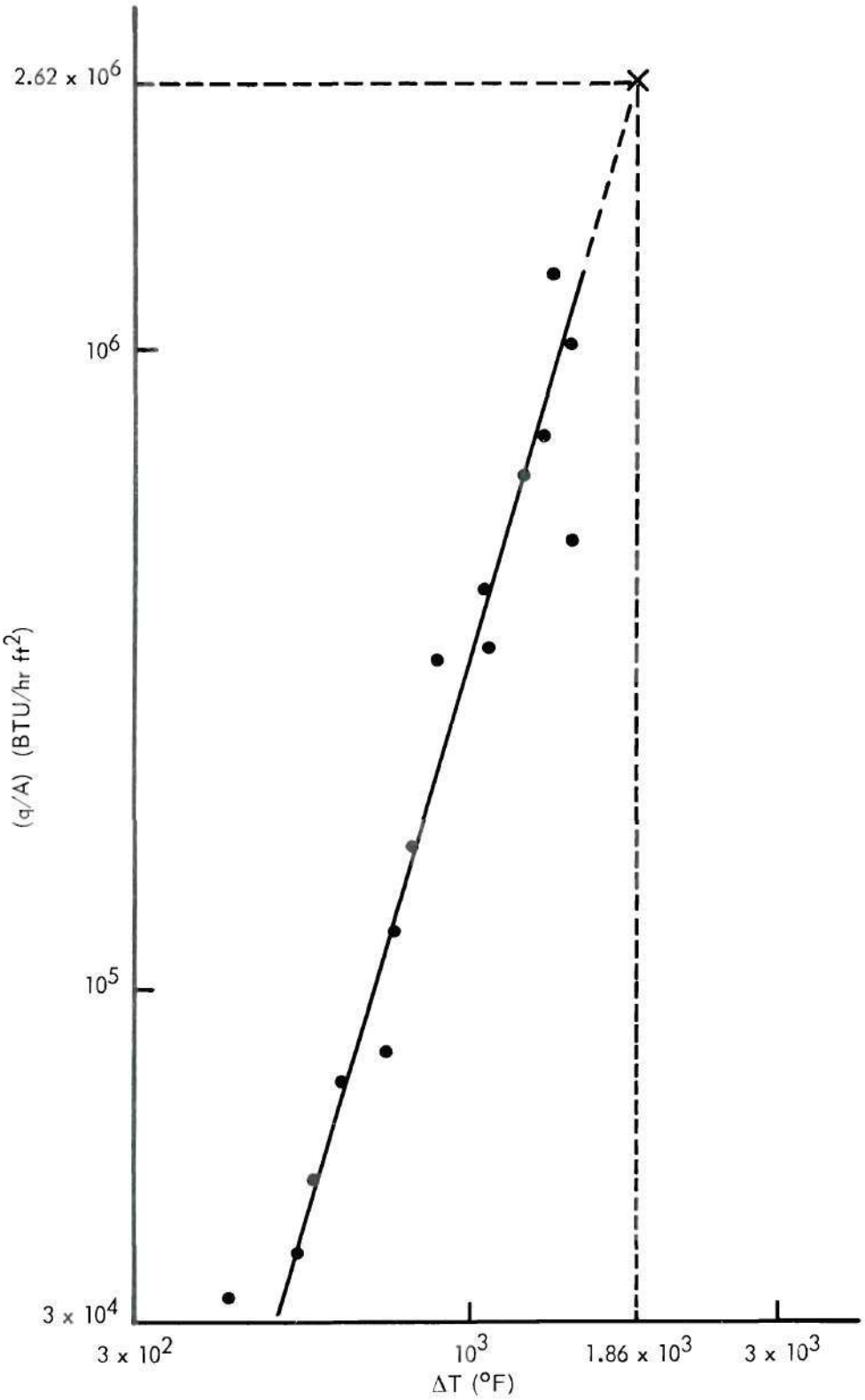

Figure 18. Heat Flux Curve for Run No. 15.

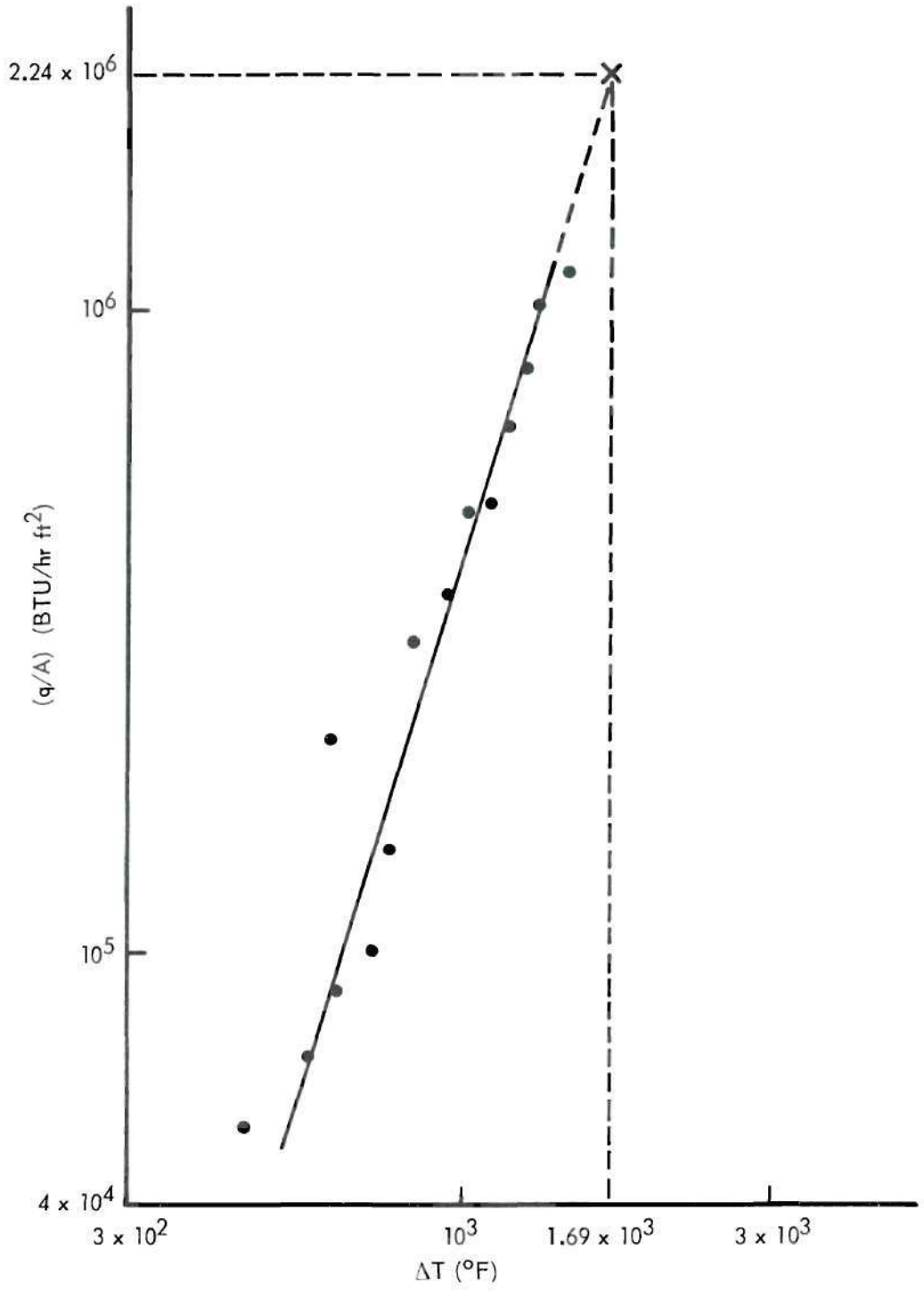

Figure 19. Heat Flux Curve for Run No. 18.

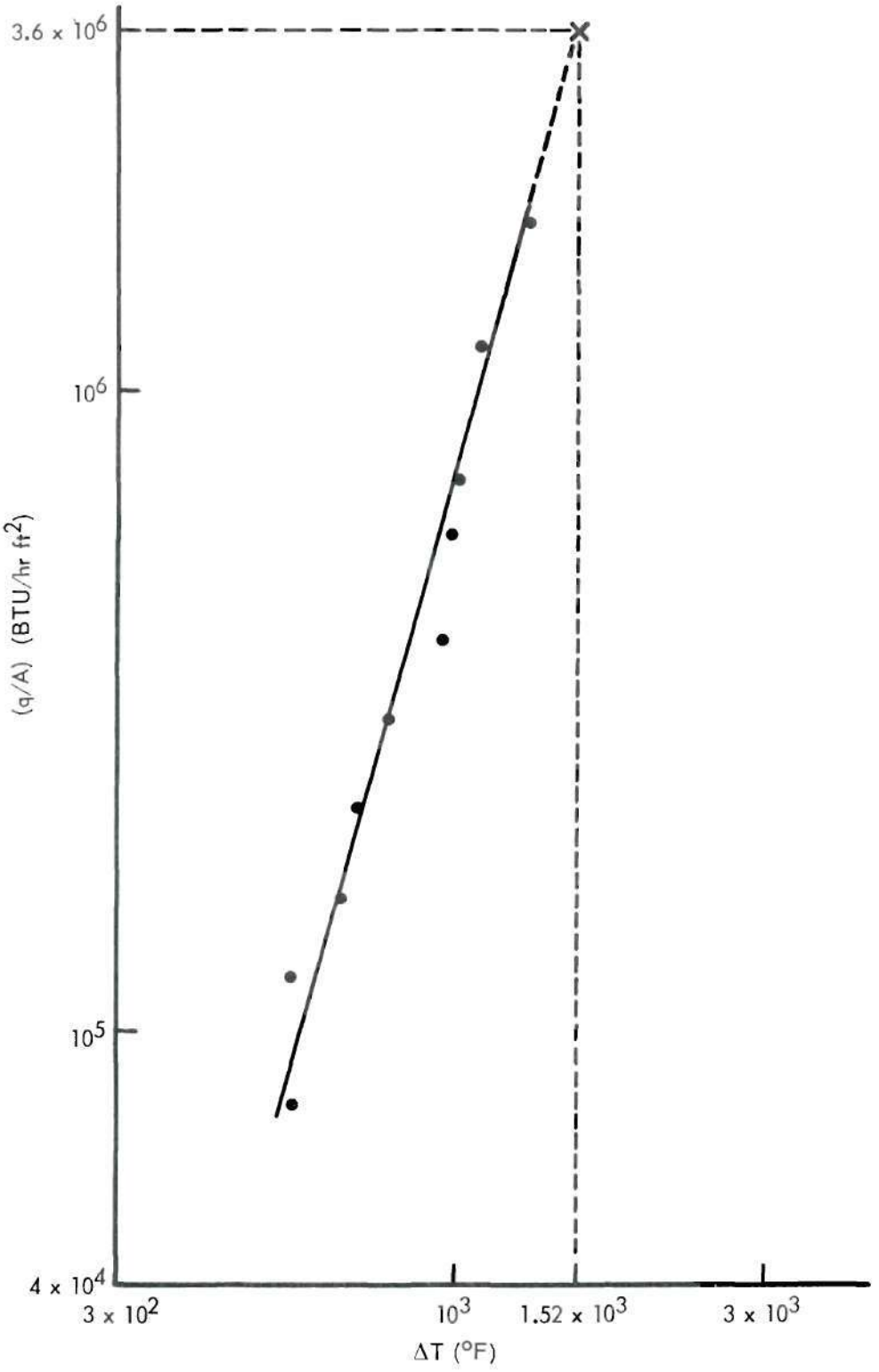

Figure 20. Heat Flux Curve for Run No. 19.

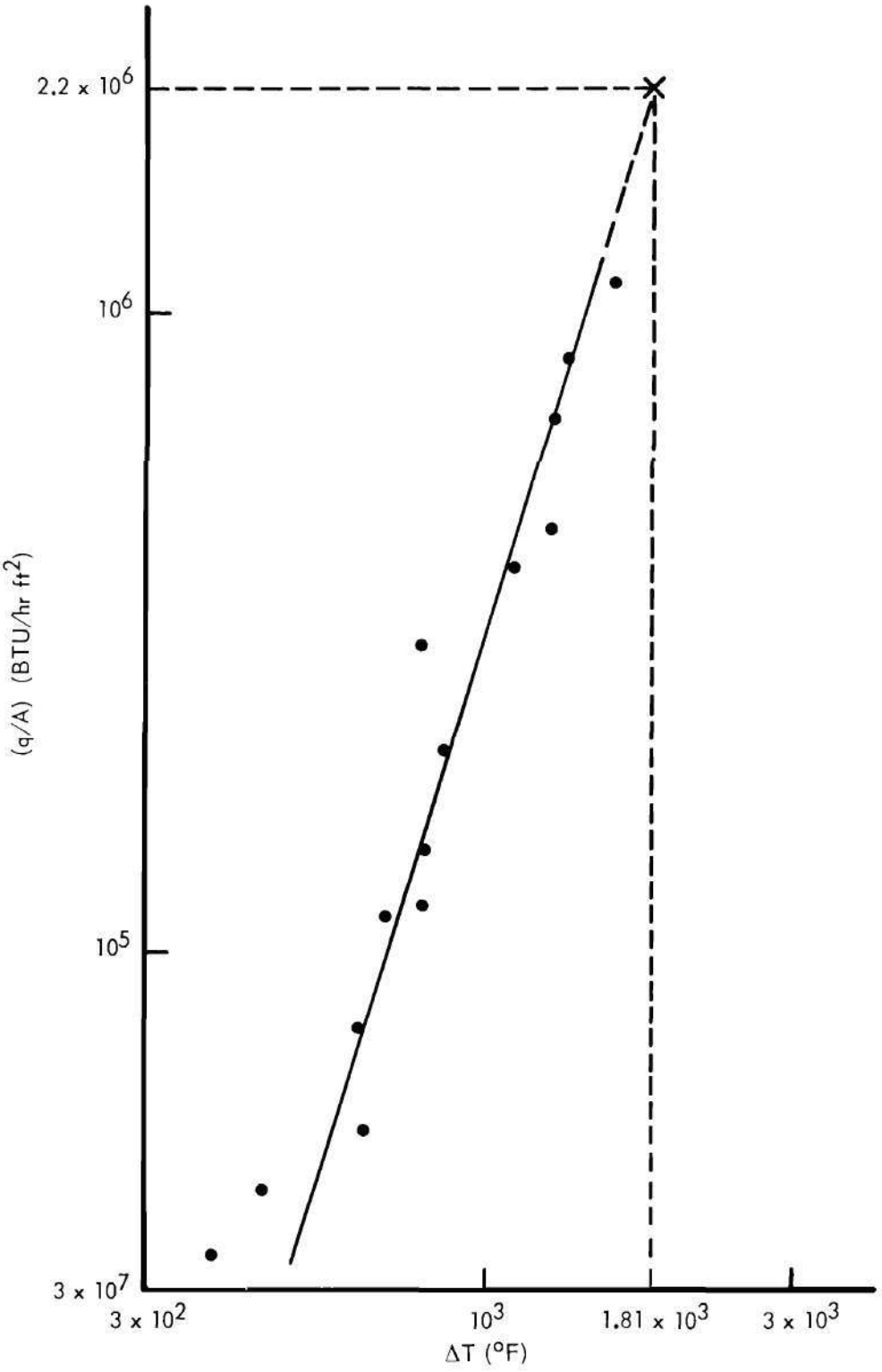

Figure 21. Heat Flux Curve for Run No. 21.

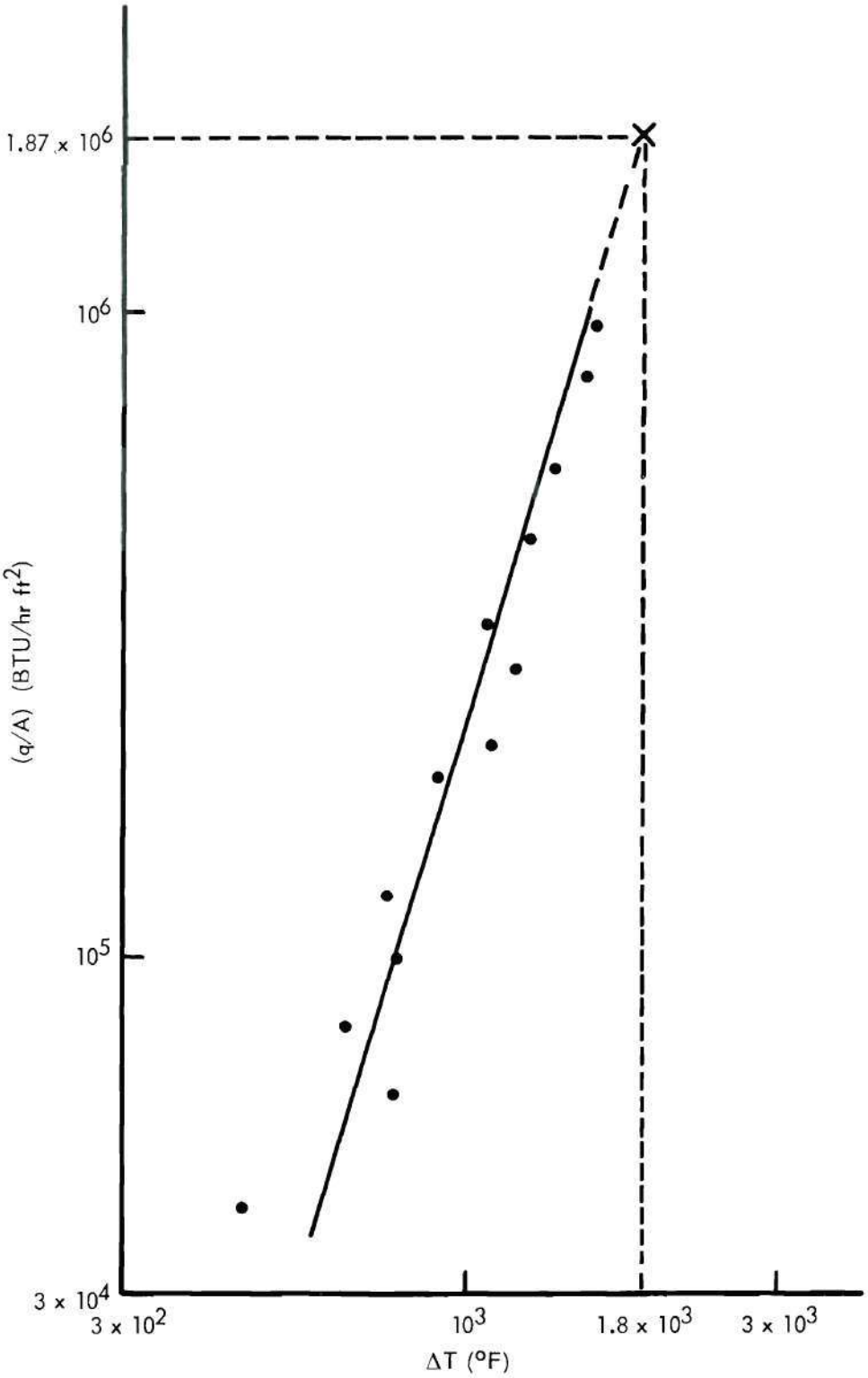

Figure 22. Heat Flux Curve for Run No. 22.

BIBLIOGRAPHY

BIBLIOGRAPHY

1. Kays, W. M., and London, A. L., Compact Heat Exchangers. Palo Alto, California: The National Press, 1955.

2. Glasstone, Samuel, Principles of Nuclear Reactor Engineering. Princeton: D. Van Nostrand Company, Inc., 1955, p. 8.

3. Holland, L., Vacuum Deposition of Thin Films. New York: John Wiley and Sons, Inc., 1956.

4. Simpson, T. B., Applications of Evaporated Metal Films. Unpublished Ph.D. Thesis, Cornell University (1954).

5. Simpson, T. B., and Winding, C. C., "Properties of Evaporated Metal Films Related to Use for Surface Temperature Measurements," Journal of the American Institute of Chemical Engineers 2, (1956), pp. 113 ff.

6. Winding, C. C., Topper, L., and Bans, B. V., "Metal-film Resistance Thermometers for Measuring Surface Temperatures," Industrial and Engineering Chemistry 47, (1955), pp. 386-92.

7. Belser, R. B., and Hicklin, W. H., Electrical Conductivity Studies of Metallic Films. Technical Report 57-660, Wright Air Development Center, (1957).

8. Hartnett, J. P., and Eckert, E. R. G., "An Experimental Study of the Velocity and Temperature Distribution in High Velocity Vortex Type Flow," Heat Transfer and Fluid Mechanics Institute Preprints, (1956), pp. 135-150.

9. Deissler, R. G., and Perlmutter, M., "An Analysis of the Energy Separation in Laminar and Turbulent Compressible Vortex Flow," Heat Transfer and Fluid Mechanics Institute Preprints, (1958), pp. 40-53.

10. Scheper, G. W., "Internal Flow Data and a Heat Transfer Theory for the Vortex Refrigerating Tube," Heat Transfer and Fluid Mechanics Institute Preprints, (1959), pp. 159-79.

11. Talbot, L., "Laminar Swirling Pipe Flow," Journal of Applied Mechanics 21, (1954), pp. 1-7.

12. Binnie, A. M., Hookings, G. A., and Kamel, M. Y. M., "The Flow of Swirling Water Through a Convergent-Divergent Nozzle," Journal of Fluid Mechanics 3, (1958), pp. 261-74.

13. Wollenberg, H., "Zur Leistungssteigerung von Rohren-apparaten," Apparatgebau 44, (1932), p. 6.

14. Nagaoka, Z., and Watanabe, A., "Maximum Rate of Heat Transfer with Minimum Loss of Energy," Proceedings of the International Congress of Refrigeration 3, (1937), pp. 221-295.

15. Kreith, F., "Heat Transfer in Curved Flow Channels," Institute of Heat Transfer and Fluid Mechanics Preprints, (1953), pp. 111-122.

16. Kreith, F., and Margolis, D., "Heat Transfer and Friction in Swirling Turbulent Flow," Institute of Heat Transfer and Fluid Mechanics Preprints, (1958), pp. 126-142.

17. Gambill, W. R., and Greene, N. D., "Boiling Burnout with Water in Vortex Flow," Chemical Engineering Progress 54, (1958), pp. 68-76.

VITA

Julian Denver Fleming, Jr., was born in Rome, Georgia, on January 12, 1934. After secondary education in the public schools of Georgia, he attended the University of Pennsylvania from 1951 to 1953 under the Alumni Regional Scholarship. In 1953 he entered the Georgia Institute of Technology where he held the Monsanto Senior Scholarship. In 1955 he was awarded the degree of Bachelor of Chemical Engineering with Highest Honor. Following graduation, he enrolled in the Graduate Division of the Georgia Institute of Technology.

Since 1955 he has held the positions of Instructor in the School of Chemical Engineering and Research Associate and Project Director in the Engineering Experiment Station of the Georgia Institute of Technology.